Semi-rigid Bolted End-Plate Moment Connections: Review and Experimental-Based Assessment of Available Predictive Models

Zizhou Ding[1] and Ahmed Elkady[2*]

[1]Doctoral student, Department of Civil, Maritime and Environmental Engineering, University of Southampton, United Kingdom

[2]Lecturer in Structural Engineering, Department of Civil, Maritime and Environmental Engineering, University of Southampton, United Kingdom ([*]*corresponding author*)

Abstract

Semi-rigid bolted end-plate moment connections are widely used in construction practice. These connections are mainly designed to resist gravity, wind, and low to moderate seismic loads. In elastoplastic designs and nonlinear system-level simulations, it is key to accurately predict/model the connection response (i.e., stiffness, strength, and ductility), rather than employing the simplified pinned/rigid idealization. Several researchers developed different empirical, analytical, and mechanical models, within the past five decades, to predict the connection's full response or key response parameters. These models are generally developed and validated based on a limited experimental and/or simulation data set; hence, their accuracy and general applicability are not well established. The potential limitations of existing models arise from the complexity of flexible connections' response due to the multitude of deforming components and the interactions between them. Accordingly, the objective of this study is to provide a comprehensive review of existing numerical models, their main assumptions and features, and to assess their accuracy. Emphasis is placed on flush and extended end-plate connections; being the most commonly used connection types. The robustness of 16 numerical models is thoroughly assessed using an experimental database, of more than 1200 specimens, that was recently collated. The assessment will demonstrate the inaccuracy of existing models in predicting the connection fundamental response quantities, particularly the elastic rotational stiffness and ductility. The advantages and disadvantages of each model are highlighted to guide future efforts to develop more accurate models in support of performance-based engineering.

Introduction

Semi-rigid beam-to-column and beam-to-beam connections are abundantly found in both conventional and ductile steel construction. In laterally-braced structures, they are typically designed to resist gravity loads only and as such, they are assumed as pinned connections. In laterally-unbraced structures, they are commonly designed to resist both gravity and lateral loads, such as those induced by wind loads and low-to-moderate earthquakes. These connections can possess moderate rotational stiffness and flexural capacity, situated somewhere between these two ideal cases of pinned (or simple) and fixed (fully rigid) connections. Bolted end-plate connections are popular worldwide, due to ease of fabrication and erection (Nethercot 1984; Kidd et al. 2016). Those come in two main configurations, flush and extended end-plate connections (referred to henceforth as FEPC and EEPC, respectively) as illustrated in Figure 1, along with key geometric parameters. These end-plate connections are characterized by a nonlinear power-shaped moment-rotation response. Their respective stiffness and strength are the highest among the different types of semi-rigid connections (e.g., shear-tab and angle connections). Properly representing the nonlinear response of semi-rigid connections can be beneficial in producing economical designs (Weynand et al. 1998; Tahir et al. 2006) as well as accurate structural responses in system-level numerical simulations.

The nonlinear response of semi-rigid connections can arise from elastic/plastic deformations taking place in more than one of the connection components (e.g., end plate bending, bolt elongation, column flange bending, column web-panel zone shear deformation). Due to the multitude of deforming components, predicting a semi-rigid connection response can be challenging. In the literature, several researchers proposed models to predict the connection response. These models can be broadly categorized as analytical, mechanical, or empirical. In analytical models, the connection response parameters (mainly the elastic stiffness and the plastic moment capacity) are computed using analytical expressions that rely on the principles of solid mechanics and material behavior. Examples of such models are the yield line method (Packer and Morris 1977) and the T-stub method (Zoetemeijer 1974); the former is demonstrated in Figure 2a. In mechanical methods, the connection components are idealized using a mechanical assembly of uniaxial springs and rigid elements; each of which represents the elastoplastic behavior of the corresponding component, as demonstrated in Figure 2b. The springs' behavior itself is generally deduced from analytical methods. The most popular application of this method is the Eurocode 3 component method (CEN 2005b). Lastly, in empirical models, regression analysis is conducted against experimental and/or simulation data to fit an empirical expression including several significant features, as illustrated in Figure 2c. These models are developed (and benchmarked) based on test/simulation data for a limited range of testing parameters (e.g., joint configuration, boundary conditions, applied load history, etc.) and connection configurations (e.g., connection geometry, materials, bolt pre-tensioning, etc.). Consequently, model extrapolation beyond the validation data set design space may yield high errors. Consequently, these models may still fall short of accurately predicting key response parameters. Moreover, analytical/mechanical models use simplified assumptions to idealize component deformation while empirical models employ a limited number of features to simplify the regression procedure and the resulting empirical expression. Consequently, not all sources of deformation as well as loading, material, and geometric parameters influencing the response are accounted for. Past brief assessments demonstrated that the error in some of these models can exceed 100%

in predicting the connection's most fundamental response parameters; the elastic stiffness and plastic strength (Benterkia 1991; Terracciano 2013).

Within the past two decades, there has been a strong push toward the development of robust numerical models and acceptance criteria for different structural components (Landolfo 2022; NIST/ATC 2018). This is driven by the growing adoption of performance-based design approaches and the rise in computational capabilities. There is also an increasing need for achieving efficient designs through the use of flexible framing to reduce construction costs and carbon emissions (Hellquist 1966; Mirza and Uy 2011; BCSA 2021; Celik and Sakar 2022). With that in mind, the first objective of this paper is to provide a thorough review of existing predictive models; their type, scope, development procedure, mathematical expressions, and limitations. This is essential given that researchers and practitioners might not be aware of many of the wide range of models in the literature. Emphasis is placed on models developed for bare steel semi-rigid end-plate moment connections with I-shaped columns and strong-axis orientation (i.e., beam connected to column flange). Models for connections with composite concrete slabs are ignored herein since the robustness of these models is eventually dependent on the ability to predict the response of the bare steel connection. The paper's second objective is to utilize a recently compiled comprehensive experimental database, comprising more than 1200 specimens, to consistently assess the accuracy of these models in predicting the connection response. This assessment will highlight the strong aspects of existing models and their drawbacks to help inform future studies aiming to develop more robust models. To the best of the authors' knowledge, this is the first study to provide a holistic review and assessment of all semi-rigid predictive models using a large experimental data set.

Existing Models for Semi-Rigid End-Plate Moment Connections

The connection's moment-rotation response is represented by different models in the literature. This includes simple linear elastic models, bilinear, trilinear, and continuous nonlinear models. In linear models, only the connection elastic rotational stiffness, K_e, is predicted. In bilinear models, K_e as well as the plastic moment M_p or the ultimate moment M_u are predicted. In continuous nonlinear models, the full moment-rotation response of the connection is predicted. Common nonlinear models are the three- (Goldberg and Richard 1963) and four-parameter (Richard and Abbott 1975) power model and the Ramberg-Osgood model (Ramberg and Osgood 1943) as given by Eqn (1) to (3), respectively and illustrated in Figure 3. The three-parameter power model requires prior knowledge of K_e and M_u. The four-parameter power model additionally requires the post-yield stiffness K_s. The Ramberg-Osgood model requires prior knowledge of the anchor point coordinates (θ_0, M_0). All these nonlinear models require a model shape parameter η that describes the transition between the elastic and plastic branches. An elaborate summary of analytical models used to represent the moment-rotation curve can be found in the literature (Abdalla and Chen 1995; Chen et al. 2011; Díaz et al. 2011; Patnana et al. 2019).

$$M = \frac{K_e\theta}{\left[1+\left(\frac{K_e\theta}{M_u}\right)^{\eta}\right]^{\frac{1}{\eta}}} \tag{1}$$

$$M = \frac{(K_e-K_s)\theta}{\left[1+\left(\frac{\theta}{\theta_o}\right)^{\eta}\right]^{\frac{1}{\eta}}}+K_s\theta \tag{2}$$

$$\theta = \frac{\theta_0}{M_0}M\left[1+\left(\frac{M}{M_0}\right)^{\eta-1}\right] \tag{3}$$

Numerous studies as well as national standards provide equations to predict the aforementioned response parameters. These models are either based on the connection kinematics and principles of solid mechanics (i.e., analytical or mechanical models) or empirically derived based on curve fitting, as discussed earlier. Analytical and mechanical models are generally robust as long as the underlying derivation assumptions are valid. However, they can be particularly laborious and generally too complex for application by practicing engineers, as well as researchers (SCI/BCSA 2013; D'Alessandro et al. 2018; Terracciano et al. 2018). This is due to the intrinsically complex elastic/inelastic behavior of semi-rigid connections, because of the multitude of deformable components within the connection (i.e., bolts, angles, plates, etc.) and the interaction between them (Steenhuis et al. 1998; Al-Aasam 2013). Empirical models, on the other hand, are advantageously simpler, making them favorable among engineers. In such models, regression analysis is conducted against a given experimental or simulation data set. The nonlinear equation, given by Eqn (4), is widely used in the literature (Benterkia 1991; Lignos and Krawinkler 2011; Lignos et al. 2019). This equation has an exponential form where *RP* is the target response parameter, X_i is feature *i* which is generally a geometric or material parameter, and c_i is the exponent for feature *i*. The exponents can be deduced from step-wise linear regression analysis in the log-log domain. On the downside, these models may lack a physical basis and, as a consequence, can sometimes lead to unrealistic numerical responses. Plus, these models are generally as good as the number of significant features considered in the regression and the size/range/quality of the data set.

$$RP = c_0\cdot(X_1)^{c_1}\cdot(X_2)^{c_2}\ \ldots\ (X_n)^{c_n} \tag{4}$$

Table 1 provides a summary of available pertinent predictive models for semi-rigid end-plate moment connections. In total there are 16 models; the majority of which (10) are either empirical or semi-empirical. These models have been in continuous development since 1975 and to the present day. Almost all these models were independently developed from each other, using different sets of experimental and/or parametric numerical simulations. In this paper, these models are assessed. Emphasized discussion is placed on the more recent predictive models and those used in European and North American design standards. Note that there are some other models available in the literature that are excluded from Table 1 and the following assessment; these are mainly 1) older models where one -or more- of the model parameters is not clearly defined in the original research or 2) models that represent a slight increment/modification to another model that is already listed in Table 1. For a detailed discussion of pre-1990 models, the reader is referred to Benterkia (1991).

Experimental Database

A comprehensive experimental database is compiled to assess the existing numerical models. The database covers both bare steel and composite end-plate connections. To date, it includes a total of 1277 test specimens collected from 176 different experimental programs conducted between 1960 and 2022. In summary, 545 are FEPCs and 732 are EEPCs. For each specimen, multiple test attributes, and geometric, and material parameters are systematically collected and tabulated. Also, the moment-rotation response is processed in digital form Figure 4 shows a summary breakdown of the database. The majority of tests involve bare steel connections comprising I-shaped columns fabricated from conventional (mild) carbon steel and subjected to monotonic loading. Most specimens are either tested in cantilever (i.e., exterior connection) or cruciform (i.e., interior connection) beam-to-column configuration while some specimens were beam-to-beam connections (i.e., splices). Also, the vast majority of beam-to-column specimens are tested with a strong (or major) axis orientation. The emphasis in this study is on these major-axis connections and associated models and not the weak-axis ones which are already limited in the literature. The database is publically available through a graphical user interface (Mak and Elkady 2021).

Deduction of Response Parameters

Figure 5 shows a typical moment-rotation curve. In the case of cyclic loading, this curve represents the average cyclic envelope (joining the peaks of the 1st cycle at each drift level) of both the positive and negative loading directions. All digitized test data are refined into 100 equally-spaced data points to ensure a consistent data fitting procedure to deduce response parameters as discussed later on. In line with existing design and numerical modeling approaches, the moment is defined as the moment at the column face, which is computed as the product of the applied force (by an actuator) or reaction force (measured by a load cell) at the beam end and the horizontal distance between the centerline of the actuator or load cell and the column flange face. The rotation is defined as the joint rotation resulting from the shear deformation of the column web, bending deformation of the column flange, plastic local deformation of the beam web/flange, elongation on the bolts, and bending deformation of the end plate. In other words, the rotation represents the total rotation of the joint minus the rotation contributions resulting from the elastic shear/flexural deformations of the beam and the column.

Key moment-rotation response parameters are deduced from the test data. This is done by fitting the response curve with a bi-linear curve as illustrated in Figure 5. The deduced parameters include the elastic and post-yield rotational stiffnesses (K_e and K_s, respectively), the yield, effective yield, maximum and capping moments (M_y, M_{ye}, M_{max}, and M_c respectively), and the maximum and failure rotations (θ_{max} and θ_f, respectively). The detailed fitting methodology is not described here for brevity but can be found in Elkady (2022). In summary, the elastic rotational stiffness K_e is deduced first followed by the post-yield stiffness, K_s, which is deduced based on the equal-area fitting method, as illustrated in Figure 5. Knowing K_s, the rest of the response parameters are obtained. This includes the effective yield moment, M_{ye}, representing the plastic moment capacity, which is deduced as the intersection point between the elastic slope and post-yield slope. Other parameters include the maximum moment, M_{max}, and the failure rotation θ_f. Another post-yield stiffness metric, $K_{s,tangent}$, is employed to represent the tangent to the post-yield region near the M_{max} point. $K_{s,tangent}$ is deduced by linear fitting one-third of the discrete data points between M_{ye} and M_{max}, that are closest to M_{max} (Elkady 2022). Consequently, M_0 is deduced as the intersection point between the elastic slope and tangent post-yield slope. These two parameters $K_{s,tangent}$, and M_0 are deduced to be able to assess existing models incorporating the four-parameter power model (refer to Figure 3b).

Assessment of Existing Numerical Models

In the following sub-sections, the accuracy of each model is assessed and possible reasons behind the model's performance are discussed. The discussion is broken into two sections, starting with analytical and mechanical models and followed by empirical models. To assess a model's accuracy in predicting a given response parameter RP, the relative error metric, $\epsilon(RP)$, is computed using Eqn (5), where RP_{test} and RP_{model} are the values of response parameter RP as deduced from the test data and predicted by the model, respectively. Accordingly, a negative error value implies a conservative model prediction and vice versa. Also, while the negative error value cannot be less than -100% (since $RP_{model} \geq 0$), the positive error value is unbounded. For models that predict the full M-θ curve directly, data fitting, as previously described, is conducted to deduce the relevant response parameters for comparison. One should note that the predicted model quantities are computed using the measured geometric and material parameters, not the nominal ones. Also, the test data subset used in the assessment excludes connections with beam haunches, atypical configurations (e.g., connections with circular bolt patterns), or those subject to bi-axial bending or dynamic loading.

The box and whiskers plot shown in Figure 6 provides a statistical summary of the observed errors in predicting the elastic stiffness and the plastic strength of both FEPC and EEPC connections for all the examined models. This figure will be cited repeatedly in the manuscript as part of the discussion. Additional scatter plots of the error metric, superimposed with the values of the associated median error (μ), will be used to further examine its distribution and bias. In these scatter plots, the ordinate representing the error will be limited to +200% to improve visuals and to exclude outliers from the discussion. The error metrics, including the error mean ($\bar{x}$), standard deviation (σ), and maximum/minimum values, are summarized in Table A.1 in the appendix. The median represents the error tendency for the majority of the predictions, the mean reflects all errors including the outliers, and the standard deviation can be used to evaluate the error variability/spread. The appendix also includes multiple comparison plots between the model predictions and reference moment-rotation data of test specimens with different configurations (see Figure A.1).

$$\epsilon(RP) = \frac{RP_{\text{model}} - RP_{\text{test}}}{RP_{\text{test}}} \times 100 \qquad (5)$$

Analytical and mechanical models

Models in design standards

The yield line method is one of the earliest analytical approaches that first emerged in reinforced concrete design (Jones and Wood 1967; Bræstrup 1970) and was later utilized in steel connection design (Packer and Morris 1977). The method assumes a plastic deformation pattern in steel plates that consists of rigid plate facets bounded by yield lines. Static equilibrium or the virtual work energy method is then used to compute the connection strength. The yield line method is used in the American design standards (Murray and Sumner 2003; AISC 2016a). The end-plate connection's plastic moment is computed as the lesser value of the end-plate and column flange plastic moments, as given by Eqn (6), where Y_{ep} and Y_{cf} are the analytically-derived yield line parameters for each component, respectively. The yield line parameter is dependent on the end-plate, column flange, bolt layout geometry, and the presence of end-plate stiffeners (ribs). The latter is typically overlooked in predictive models. Those expressions are assessed herein.

In addition to the yield line method's idealization of the deformed shape of plates in bending, the expressions are deduced assuming an end plate and beam flange of equal widths. In fact, AISC Design Guide 16 (Murray and Shoemaker 2002) specifies that the effective end plate width shall not be taken larger than the beam flange width plus one inch. While this is typically the case in practice, there are several situations where the end plate can be up to twice the beam flange width (Thomson and Broderick 2002; Rölle 2013). For those, the yield line patterns may diverge from those assumed. Furthermore, the yield line method does not consider deformation modes other than end-plate and column flange bending. While these two deformation modes are the most common (Elkady 2022), in stiffened connections (i.e., with continuity plates) employing thick end-plates (t_{ep} ≥40mm) and/or relatively slender beams, plastic strength is controlled by bolt rupture or beam flange/web buckling. These cases are excluded from the data used in Figure 7 which shows the error with respect to the deduced M_{ye}. The yield line parameters are computed based on Eatherton et al. (2021) who recently deduced and summarized the expressions for FEPCs and EEPCs with different configurations.

$$M_{\mathrm{p}} = \min \begin{cases} f_{\mathrm{y,P}} \cdot t_{\mathrm{ep}}^2 \cdot Y_{\mathrm{ep}} \\ f_{\mathrm{y,C}} \cdot t_{\mathrm{cf}}^2 \cdot Y_{\mathrm{cf}} \end{cases} \tag{6}$$

On average, the yield line model strength estimates are adequate for both connection types, with a median error of +2%. The error is almost normally distributed with most errors falling within the ±50% range. Although this is still a large error, it is reasonable considering the simplicity of the model and its closed form that is easily applied in practice. No bias is observed between the model error and the controlling component (deformation mode) as demonstrated in Figure 8a for EEPCs. However, a negative correlation is observed between the error and the ratio of the beam depth to the end plate thickness (or the column flange thickness if it is the controlling component) as shown in Figure 8b. Essentially, the yield line model tends to overpredict the strength of connections with shallow beams and thicker end plates and provides reasonable strength estimates of those with deep beams and thinner end plates. This is expected given that the latter case involves thin plates that generally deform per the assumed yield patterns (with narrow-banded and clearly-defined yield lines). Correlation plots like the one shown in Figure 8b can be used to potentially develop empirical correction factors to reduce the error of this model. In addition to the aforementioned model assumptions, part of the observed –overestimation- errors arise from the fact that different yielding patterns can be used to deduce the yield line parameter. Ideally, the pattern that yields the smaller Y shall be used, however, this can be dependent on the connection geometry (e.g., the extension length e_t). For practical reasons, however, only patterns that are shown to match experimental data best are recommended in the literature. This means that errors can occur in some other cases.

In this model and subsequent models, part of the error can be attributed to the uncertainty in the employed response parameter definitions, based on the prescribed curve fitting methodology (refer to Figure 5). For example, M_{ye} is used in the assessment above instead of M_0, though both represent the plastic strength. This uncertainty was checked for different strength/stiffness metrics and it was noted that the variation in the response parameter definition does not contribute more the ±8% to the observed errors.

In 2005, Eurocode 3 Part 1-8 (CEN 2005b) (referred to henceforth as EC3) incorporated the "component method" for the design and analysis of steel joints. This method is widely recognizable and comprises a detailed and comprehensive mechanics-based procedure in which the strength and stiffness parameters associated with each of the connection individual components' deformation/failure modes are computed based on analytical expressions and then assembled to generate the global response. The method relies on the equivalent T-stub model that is used to represent the bending behavior of the column flange and the end plate (Zoetemeijer 1974; Jaspart 1991; Weynand et al. 1996). The joint's plastic resistance ($M_{j,Rd}$) and initial rotational stiffness ($S_{j,ini}$) are computed based on Eqns (7a) and (7b), respectively, where F_{row} and z_{row} are the tensile resistance of a given bolt row and its corresponding lever arm from the center of compression, respectively, E is the steel elastic modulus, z is the equivalent lever arm and k_i is the stiffness factor for component i. Using these two parameters, the M-θ response can be established as shown in Figure 9. The complete analytical expressions to compute F_{row} and k_i are not shown here for brevity.

$$M_{j,Rd} = \sum_{row} F_{row} \cdot z_{row} \tag{7a}$$

$$S_{j,ini} = \frac{E \cdot z^2}{\sum_i \frac{1}{k_i}} \tag{7b}$$

This method is generally considered complex and laborious, prompting engineers to opt for the simplified pinned/rigid connection assumption; thereby forfeiting the advantages of semi-rigid connections. Excluding this issue, past studies showed that this method is capable of predicting the connection controlling failure mode (Thomson and Broderick 2002; Hettula 2017) and can provide an acceptable conservative estimate of the connection flexural strength (Coelho and Bijlaard 2007; Terracciano et al. 2018). Others showed that it can under-predict the flexural strength by up to 55% (Thomson and Broderick 2002; Hettula 2017). Notably, most studies showed that it fails in predicting the elastic stiffness, mostly yielding estimates that are larger than three times the measured stiffness; i.e., $\epsilon > +200\%$ (Brown 1995; Thomson and Broderick 2002; Heong 2003; Liew et al. 2004; Coelho and Bijlaard 2007; Hettula 2017; Terracciano et al. 2018; Gao et al. 2020; Gao et al. 2021).

EC3 is used herein to predict $M_{j,Rd}$ and $S_{j,ini}$ for bare steel specimens with I-shaped columns. Unit values are assumed for the partial safety factors and measured material properties are considered. Figure 10 shows the error in predicting $M_{j,Rd}$ and $S_{j,ini}$ relative to the deduced moment at 1/3 K_e (i.e., the intersection of the secant stiffness (1/3 K_e) with the test moment-rotation curve, consistent with the $M_{j,Rd}$ definition in Figure 9) and K_e, respectively, as well the corresponding error histogram distributions. The dataset plotted in this figure includes both beam-to-column and beam-to-beam bare steel connections with I-shaped members and major-axis orientation. Furthermore, since the component method did not exhibit any bias in the observed prediction errors with respect to connections with stiffened and unstiffened columns (or other connection characteristics), no distinction is made in the plot between the different cases.

No tendency is observed in FEPCs' strength predictions which are slightly conservative with a median error of -9%. On the other hand, for EEPCs, the component method underestimates the strength by about -20%. For both connection types, the median and mean error values are close; implying that the error is normally distributed with a standard deviation of about ±33% which is relatively narrow. Hence, as a temporary fix, applying an amplification factor of 1.09 and 1.20 to EC3 FEPC and EEPC strength predictions, respectively, would help translate the median error to zero. Excluding the limited cases with outliers, the error in the majority of predictions falls within ±50%. Granted that part of this error might be attributed to the uncertainty associated with the reported geometric and material test parameters, the error is still significant. It is worth noting that the error scatter remains practically the same if $M_{j,Rd}$ is compared to M_{ye} instead of the moment at one-third of the elastic stiffness, as per Figure 9. This means that this error is not a result of the uncertainty associated with the method used to deduce the plastic strength from the test data. Generally, the observed errors can be attributed to the assumptions of the component method, particularly, the T-stub approach and yield line mechanism. This approach considers three discrete T-stub modes of deformations and effective T-stub lengths that are based on pre-defined and idealized yield patterns. The method also assumes the center of the beam compression flange as the connection's center of rotation, which is then used to compute the lever arm for the different bolt rows. This is a major assumption given that the center of rotation is dependent on the end plate's deformed shape, which is dependent on its thickness and the bolt layout. Relatively large errors are also observed in test specimens with uncommon configurations such as FEPCs with uncommonly large bolt gauge-length (g) (Zoetemeijer 1981), EEPCs with four bolts per row, two bolt rows in the extended end-plate portion, stiffened end-plates, and deep beams (h_b >700mm). It is worth noting that model amendments for 4 bolt per row connections are employed herein as proposed in Demonceau et al. (2010) and validated against tests conducted by Ungermann et al. (2009) for splice connections. Although the component method is supposed to be generally applicable, these connection configurations are outside the common design range considered in the development of the method. Also, EC3 ignores strain hardening and membrane effects.

Referring to Figure 10c-d, similar observations are inferred concerning the initial rotational stiffness. In particular, the component method tends to overestimate K_e by an average of 35%, consistent with prior studies. Most importantly, significant variability is observed in the stiffness predictions, with an error standard deviation larger than ±150%. There was no observed correlation between the error values and the joint configuration or with any key geometric parameters such as h_b/t_{ep} or t_{ep}/t_{cf}. For K_e, the EC3 component method still overlooks several model parameters such as the bolt pre-tension force, the axial load demand in the beam and column, and the shear-to-moment ratio in the connection. Contrary to the plastic strength which is controlled by the main yielding component, the elastic stiffness is a particularly sensitive response parameter that is affected by all of the connection's deforming components. It will be demonstrated herein that large K_e errors with large variability are observed in all models' predictions (refer to Figure 6a).

Simplified analytical models

Several simplified analytical models have been proposed as an alternative to the yield line and component methods. These are either pure analytical models or hybrid models that employ analytical expressions modified by empirically-driven coefficients for further simplification or improved accuracy. Four of these models are discussed herein.

Brown et al. (2001) developed analytical expressions to compute the initial rotational stiffness of FEPCs and EEPCs. These expressions explicitly account for the column flange and the end plate flexibility in bending as well as the column web deformation in shear. Other sources of flexibility are implicitly considered using a correction factor for simplification. The equivalent connection stiffness is computed using Eqn (8) by assembling the individual component stiffnesses based on the mechanics-based component method that was introduced in Annex J of EN1993-1:1998 (CEN 1998). The model was validated against 16 test specimens; all of which have standard configurations (i.e., 4-bolt FEPCs and 8-bolt EEPCs) and end-plate thicknesses less than 16mm. The model provides highly conservative estimates of K_e that are 45% to 60% lower than the true value, as shown in Figure 11a. Although not demonstrated in the figure, no difference was observed between stiffened and unstiffened connections or between those with a standard configuration and others. Compared to other models, these conservative predictions are coupled with low error standard deviation (σ=±57), particularly for EEPCs. Hence, an amplification factor of about 1.6 can be used to improve the overall model predictions. The main drawback of this model is the exclusion of the bolt stiffness and its pre-tension force (degree of contact between the end-plate and the column flange) as well as the exclusion of the axial load effect and the bending flexibility of the column web (Skiadopoulos et al. 2021). These significant predictors are regularly ignored in the assessed models.

$$K_{\mathrm{j}} = \frac{0.2 l_{\mathrm{a}}^2}{\left(\frac{m_{\mathrm{cf}}^2}{t_{\mathrm{cf}}^3} + \frac{m_{\mathrm{ep}}^2}{t_{\mathrm{ep}}^3} + \frac{\beta l_{\mathrm{a}}}{0.38 A_{\mathrm{vc}}} \right)} \tag{8}$$

Where,

$$m_{\mathrm{cf}} = \frac{g}{2} - \frac{t_{\mathrm{cw}}}{2} - 0.8 r_{\mathrm{c}} \quad m_{\mathrm{ep}} = \begin{cases} g/2 - t_{\mathrm{bw}}/2 - 0.8 t_{\mathrm{weld}} & \text{FEPC} \\ p_{\mathrm{t}} + e_{\mathrm{rt}} - e_{\mathrm{t}} - t_{\mathrm{bf}} - 0.8 t_{\mathrm{weld}} & \text{EEPC} \end{cases} \quad l_{\mathrm{a}} = \begin{cases} h_{\mathrm{b}} - e_{1} - t_{\mathrm{bf}}/2 & \text{FEPC} \\ h_{\mathrm{b}} - t_{\mathrm{bf}}/2 & \text{EEPC} \end{cases} \tag{8a}$$

Guo et al. (2011) also developed a simple analytical model to predict the elastic stiffness of EEPCs. The model considers the equivalent flexibility of the end plate in bending (K_{epb}) and the column panel zone in shear (K_{cws}), as given by Eqn (9). The model was validated against only three tests involving 8 bolts and stiffened class 3 columns; hence, column flange deformations are ignored. This model is a simplified version of the Brown et al. (2001) model. Therefore, similar observations are made with respect to K_{e} predictions being conservative and inconsistent as shown in Figure 11b. Moreover, due to this further simplification (i.e., the exclusion of column flange bending), the model provides larger variability in prediction with an error standard deviation of ±111% (compared to +57% for Brown et al. (2001) model). No bias is observed with respect to stiffened/unstiffened connections or with respect to specimens that were controlled by different deformation modes.

$$K_{\mathrm{e}} = \frac{K_{\mathrm{epb}} \cdot K_{\mathrm{cws}}}{K_{\mathrm{epb}} + K_{\mathrm{cws}}} \quad \text{where, } K_{\mathrm{epb}} = \frac{6 E_{\mathrm{p}} I_{\mathrm{ep}} h_{\mathrm{b}}^{2}}{e_{\mathrm{f}}^{3}} \text{ and } K_{\mathrm{cws}} = G(h_{\mathrm{b}} - t_{\mathrm{bf}}) h_{\mathrm{c}} t_{\mathrm{cw}} \tag{9}$$

Most recently, Kong et al. (2020) developed a hybrid mechanical/empirical model to predict the elastic stiffness and ultimate moment of FEPCs. The model is developed based on a data set of 46 test specimens. For predicting K_{e}, the model employs Eqn (9), similar to Guo et al. (2011). The only difference here is that the effective end-plate bending length, e_{f}, is empirically estimated based on regression analysis against the collected test data, as given by Eqn (11b). For predicting M_{u}, the model considers the end-plate yield line mechanism in bending as observed from four validated FE simulations based on the tests by Qiang et al. (2014). The effect of shear-moment interaction is also considered as per Drucker (1956) yield criterion, as given by Eqn (11b). Note here that the model defines M_{u} as the moment capacity at a joint rotation of 3% as per AISC (2016b) unless failure occurred earlier.

Figure 12 shows the error scatter for K_{e} and M_{u} with respect to the corresponding deduced test parameters. Although the scatter differentiates between connections with stiffened and unstiffened columns, the model does not. The model is on the conservative side as it underestimates K_{e} by 51% and 24% for connections with stiffened and unstiffened columns, respectively. The much lower K_{e} values for stiffened connections are expected considering that the model does not consider the stiffeners' effect on the connection flexibility. Consistent with all the other models so far, high variability is observed in the K_{e} predictions with errors mostly falling between ±100%. These observations are consistent with those of the model's authors who reported errors of up to -44% based on the test data set used in the model development.

Based on Figure 12b, the model does a relatively reasonable job predicting M_u for stiffened connections with most errors falling between ±25%. This is consistent with the model's authors' reported discrepancies that varied roughly between -30% and +40%. For unstiffened connections, large errors reaching +200% are observed with significant scatter. This is attributed to the fact that the yield line mechanism will change if the connection geometry and bolt layout are different from the reference 4- and 6-bolt connections used to develop this model. The model M_u predictions are also better for connections with relatively thin end-plate ($t_\mathrm{ep}/t_\mathrm{cf}$ < 1). The error increases substantially with thicker end-plate as demonstrated in Figure 13, particularly for unstiffened connections. This is because, in such connections, the column web-panel zone in shear and the bolt elongation in tension control the connection deformation.

$$M_\mathrm{u} = 2\left[\frac{\left(2V_\mathrm{ep,u} + V_\mathrm{ep,0}\right)}{6}\left(h_\mathrm{ep} - l_\mathrm{c}^{2}\right) + V_\mathrm{ep,u} l_\mathrm{c}\left(h_\mathrm{ep} - \frac{l_\mathrm{c}}{2}\right)\right] \tag{10}$$

Where,

$$\begin{aligned} &e_\mathrm{f} = e^{-13.9646}\cdot\left(g^{0.9}\cdot(e_1 - t_\mathrm{bf}/2)^{0.3}\cdot t_\mathrm{ep}\right)^2 + e^{-4.8283}\cdot g^{0.9}\cdot(e_1 - t_\mathrm{bf}/2)^{0.3}\cdot t_\mathrm{ep} + 32.11 \\ &l_\mathrm{c} = e_\mathrm{f} + e_\mathrm{rt} + t_\mathrm{bf}/2 \\ &\left(\frac{V_\mathrm{ep,u}}{V_\mathrm{ep,0}}\right)^4 + \frac{g}{2t_\mathrm{ep}}\left(\frac{V_\mathrm{ep,u}}{V_\mathrm{ep,0}}\right) - 1 = 0.0 \end{aligned} \tag{11b}$$

Empirical models

In this section, empirical models are assessed. Those are divided into two categories based on the data type used in developing the model; specifically, a) data generated by the EC3 component method or b) data obtained from physical tests and/or FE simulations. In total ten models are assessed; two based on the first category and eight based on the second category.

Models driven by EC3 component method

Following the commissioning of the EC3 component method, there has been an ongoing effort to develop a simpler alternative to the method's lengthy and complex computations. The earliest was the empirical equations developed by Kozlowski et al. (2008) to predict the initial rotational stiffness and plastic strength of both bare steel and composite beam-to-column connections. These equations were developed by regressing parametric data that are generated using the EC3 component method procedures, rather than experimental data. The parametric data considered connections with European IPE160 to IPE400 beams, HEB140 to HEB400 beams, Grade 10.9 M16 to M24 bolts, and t_{ep} between 12mm and 30mm. Different equations are developed for different connection configurations (interior/exterior connections with stiffened/unstiffened columns); those for FEPCs are given by Eqns (11a-b). The equations have a simplified form with only four geometric features; the column depth, the beam depth, the end-plate thickness, and the bolt diameter. No material parameters are considered nor does the model account for the bolt pretension force or the presence of end-plate (rib) stiffeners in EEPCs.

Similar to the EC3 component method, the model K_e predictions are mostly overpredicted, inconsistent, and yield excessive errors across all different connection configurations; though the model tends to be more accurate for interior stiffened connections (see Figure 14a). Higher errors, compared to EC3, are observed in this model because of the regression simplifications. As for the plastic strength, the model provides good conservative predictions for FEPCs with a median error of about -9% as shown in Figure 14b. The model also provides consistent predictions for specimens that fall within and outside the model's range of applicability (refer to Figure 6). The error variability is comparable to that of the EC3 model. As such, this model can be considered a faster and more efficient alternative to the component method, which can be helpful when in the early stages of frame design calculations.

$$M_{\mathrm{p,Rd}} = \begin{cases} e^{-11.1765} \cdot h_{\mathrm{c}}^{0.09} \cdot h_{\mathrm{b}}^{1.7} \cdot t_{\mathrm{ep}}^{0.63} \cdot d_{\mathrm{b}}^{1.1} + 7 & \text{interior \& unstiffened} \\ e^{-9.9869} \cdot h_{\mathrm{c}}^{0.35} \cdot h_{\mathrm{b}}^{1.5} \cdot t_{\mathrm{ep}}^{0.49} \cdot d_{\mathrm{b}}^{0.81} & \text{exterior \& unstiffened} \\ e^{-10.2892} \cdot h_{\mathrm{c}}^{-0.05} \cdot h_{\mathrm{b}}^{1.77} \cdot t_{\mathrm{ep}}^{0.63} \cdot d_{\mathrm{b}}^{0.98} & \text{interior/exterior \& stiffened} \end{cases} \tag{11a}$$

$$S_{\mathrm{j,ini}} = \begin{cases} e^{-2.0402} \cdot h_{\mathrm{c}}^{-0.32} \cdot h_{\mathrm{b}}^{2.3} \cdot t_{\mathrm{ep}}^{0.51} \cdot d_{\mathrm{b}}^{-0.13} - 6261 & \text{interior \& unstiffened} \\ e^{-4.4228} \cdot h_{\mathrm{c}}^{-0.38} \cdot h_{\mathrm{b}}^{2.6} \cdot t_{\mathrm{ep}}^{0.60} \cdot d_{\mathrm{b}}^{-0.03} + 1074 & \text{exterior \& unstiffened} \\ e^{-3.3382} \cdot h_{\mathrm{c}}^{-0.4} \cdot h_{\mathrm{b}}^{2.5} \cdot t_{\mathrm{ep}}^{0.75} \cdot d_{\mathrm{b}}^{0.042} - 5377 & \text{interior/exterior \& stiffened} \end{cases} \tag{11b}$$

More recently, acknowledging the laborious and lengthy procedures of the EC3 component method, Terracciano et al. (2018) conducted a parametric study using the EC3 component method to generate ready-to-use 2-dimensional contour plots (i.e., design charts) to graphically determine the connection stiffness and strength. Simplified empirical equations were also developed, as given by Eqns (12a-b). The parametric study involved standard European EEPCs with 8-bolt configuration, stiffened columns, and assuming equal end-plate and column flange thicknesses. The equations are a function of the bolt diameter, the column flange thickness, and the column and beam depths. Although t_{ep}=t_{cf} is assumed in this model, a more logical choice here would have been using t_{ep} instead of the t_{cf} in the equation. This would better reflect the response variation in specimens outside this assumption, where end plate deformation is typically dominant. As expected, in regards to K_e, this model performance is similar to the EC3 component method, with large variation in predictions (see Figure 15a), though this model underpredicts K_e by about 20% contrary to EC3 which tends to overestimate it. One should note that no bias is observed between connections falling within (solid black markers in Figure 15) or outside the model's applicability range. The model overestimates M_p significantly by about 48% which is comparable to EC3 (μ=+53%) (see Figure 15b). The model shows an improvement is observed for M_p prediction for specimens within the applicability range, where the error values become more consistent and the median error is about +30%. This is more or less consistent with Terracciano et al. (2018) observations where M_p predictions are 7% smaller than the that of EC3 method. It is worth noting that Kozlowski et al. (2008) model does a better job predicting the plastic strength of FEPCs compared to this model's predictions for EEPCs. This may be attributed to the more complex behavior of EEPCs compared to FEPCs, particularly when it comes to the moment lever-arm assumption. In that respect, this model is valid as a simpler alternative to the EC3 component method, as long as it is used within the range of applicability.

$$K_e = \left[8.343 \cdot \left(\frac{d_b}{t_{cf}} \right)^3 - 33.3 \cdot \left(\frac{d_b}{t_{cf}} \right)^2 + 47.32 \cdot \left(\frac{d_b}{t_{cf}} \right) + 0.865 \right] \cdot \left(\frac{k_{b,1.5}}{25} \right) \cdot (EI_{x,b} / L_b)$$
$$\text{where, } k_{b,1.5} = \alpha_k \cdot h_b + \beta_k \qquad (12a)$$
$$\alpha_k = \text{-}1.35 \times 10^{-6} \cdot h_c^2 + 1 \times 10^{-3} \cdot h_c - 0.188$$
$$\beta_k = 12.39. \times 10^{-4} \cdot h_c^2 - 0.19 \cdot h_c + 53.12$$

$$M_p = \begin{cases} \left[2.205 \cdot \left(\frac{d_b}{t_{cf}} \right) - 0.524 \right] \cdot m_{b,1.5} \cdot (Z_{x,b} \cdot f_y) \le m_{b,1.5} & \text{for } h_c \le 160\text{mm} \\ \left[1.690 \cdot \left(\frac{d_b}{t_{cf}} \right) - 0.371 \right] \cdot m_{b,1.5} \cdot (Z_{x,b} \cdot f_y) \le m_{b,1.5} & \text{for } h_c \ge 180\text{mm} \end{cases}$$
$$\text{where, } m_{b,1.5} = \alpha_m \cdot h_b + \beta_m \qquad (12b)$$
$$\alpha_m = \begin{cases} \text{-}1.404 \times 10^{-7} \cdot h_c^2 + 9.466 \times 10^{-5} \cdot h_c - 0.0169 & \text{for } h_c \le 310\text{mm} \\ 9.282 \times 10^{-4} & \text{for } h_c \ge 340\text{mm} \end{cases}$$
$$\beta_m = \begin{cases} \text{-}5.799 \times 10^{-3} \cdot h_c + 3.142 & \text{for } h_c \le 310\text{mm} \\ 0.003 \cdot h_c + 0.344 & \text{for } h_c \ge 340\text{mm} \end{cases}$$

Models driven by test and/or simulation data

Among the earliest forms of nonlinear models is the odd-power polynomial model given by Eqn (13), where c and k parameters are the model constants and standardization factor, respectively. This empirical model was developed by Frye and Morris (1975) and is built on prior work by Sommer (1969) on header-plate connections, to predict the response of bare steel beam-to-column interior (cruciform) connections. The model coefficients were calibrated using 30 specimens from early test data by Johnson et al. (1960), Sherbourne (1961), and Ostrander (1970). The model considers the end-plate and the column flange thicknesses, the distance between the extreme bolt rows as well as the presence of column stiffeners as given by Eqn (13a).

Figure 16 shows the error scatter for K_e and M_{ye} for both FEPCs and EEPCs. In this plot, splice connections as well as connections with special configurations involving 4 bolts per row or 2 bolt rows in the extended end-plate portion are excluded. The figure shows that the model consistently and significantly underpredicts the *M*-*θ* curve of stiffened FEPCs (see sample comparisons in the appendix). In particular, K_e and M_{ye} are underpredicted by about 87%. Obviously, a simple amplification correction factor of 1.87 would help alleviate the model error for stiffened FEPCs. For stiffened EEPCs, the model conservatively predicts a plastic strength that is 42% lower than observed. Similarly, an amplification correction factor of 1.42 would help move the median error to zero. For all other types of connections, the model exhibits significant error and large variability in predictions, particularly for the stiffness. This is consistent with past observations by Benterkia (1991). This can be attributed to the limited number of features considered by the model. For instance, the model does not account for the material strength, the bolt size, the bolt rows pitch, the shear, and axial load effects, or the column panel zone deformation; all of which are influential parameters. The model also does not differentiate between FEPCs and EEPCs, although their response is different particularly in regards to the deformation mode of the end plate. Furthermore, this model is regarded in the literature as unfavorable as it can produce unrealistic negative stiffness because of the negative exponents, with respect to the rotation.

To improve the model accuracy for EEPCs, subsequent research (Goverdhan 1984; Benterkia 1991) suggested replacing the z_{ex} parameter with the beam depth, h_b, and the associated -2.4 exponent with -2.6. These modifications only improve the plastic strength predictions for stiffened FEPCs where the median error is shifted from -87% to +15%.

$$\theta = c_1(kM) + c_2(kM)^3 + c_3(kM)^5 \qquad \text{units: inches, kip.in} \tag{13}$$

Where,

$$\begin{aligned} &c_1 = 1.83\times10^{-3},\ c_2 = -1.04\times10^{-4},\ c_3 = 6.38\times10^{-6},\ k = z_{\mathrm{ex}}^{-2.4}\cdot t_{\mathrm{ep}}^{-0.4}\cdot t_{\mathrm{cf}}^{1.1} \quad \text{unstiff.} \\ &c_1 = 1.79\times10^{-3},\ c_2 = 1.76\times10^{-4},\ c_3 = 2.04\times10^{-4},\ k = z_{\mathrm{ex}}^{-2.4}\cdot t_{\mathrm{ep}}^{-0.6} \quad \text{stiff.} \end{aligned} \tag{13a}$$

More than a decade later, Kukreti et al. (1987) developed a two-parameter power model (see Eqn (15)), to predict the response of 4-bolt bare steel splice FEPCs under symmetric loading (i.e., equal bending). Regression analysis was conducted to find the features' exponents as given by Eqn (14a). This was based on 50 two-dimensional parametric FE simulations that were validated against 8 splice tests by Srouji (1983).

The model considers the beam, end-plate, and bolt dimensions, geometric layout, as well their respective material properties. In total, 12 features are considered in normalized form. The model is valid for small rotations within the elastic phase; hence, it can be used to estimate the elastic rotational stiffness, K_e. Furthermore, as the model is developed for splice connections, it does not take into account the column deformations and consequently, it does not apply to beam-to-column connections. Nonetheless, its applicability is investigated here for cruciform (interior) beam-to-column connections with stiffened columns where column deformations are already limited.

Figure 17 shows the error in predicting K_e for splice and stiffened interior connections. For the splice tests by Srouji (1983) that were used in model development (highlighted by red markers), the model appears to provide reasonable collective error that is centered around zero; though most K_e predictions are underpredicted by about 19%. This is consistent with the original research observations of a -5 to -20% difference, which was deemed adequate at that point given the complexity of the problem. Beyond this set, K_e is largely overpredicted by a factor of three on average. Large errors are particularly observed in splice connections with four bolts per row and in those subjected to beam axial load (Wald and Švarc 2001; Ungermann et al. 2009). For stiffened cruciform connections, relatively high stiffness is also predicted. This is expected given that column deformations are ignored. More importantly, the predictions, in this case, are largely inconsistent and a substantial variability is observed in the error ($\sigma = \pm 361$). This can be attributed in part to the limited number of tests used to develop this model; resulting in extrapolation errors. This is highlighted in Figure 17b, which shows the correlation between the error and the end plate thickness. In this figure, relatively lower errors are observed for thinner end plates that are similar to those tested by Srouji (1983) (t_{ep}=9 to 13mm), while the errors tend to increase with thicker plates.

$$\theta = 1.5 \cdot c \cdot \frac{M^{1.356}}{h_b} \quad \text{units: inches, kip.ft} \tag{14}$$

Where,

$$c = e^{-8.335}\left(\frac{t_{ep}}{h_b}\right)^{7.62}\left(\frac{p_f}{h_b}\right)^{-6.93}\left(\frac{t_{bw}}{h_b}\right)^{-0.50}\left(\frac{t_{bf}}{h_b}\right)^{-0.032}\left(\frac{b_{ep}}{h_b}\right)^{2.89}\left(\frac{d_b}{h_b}\right)^{-0.85}\left(\frac{1}{3}\frac{f_{y,B}}{f_{y,b}}\frac{A_b}{d_b}\right)^{-0.52}\left(\frac{p_f^3}{b_{ep}t_{ep}^3}\right)^{3.05} \tag{14a}$$

Benterkia (1991) compiled an experimental database of pre-1990s research and used it to develop an empirical model to predict the nonlinear moment-rotation response of FEPCs, using Eqn (15). The model is developed for unstiffened connections with up to two bolt rows in tension and is valid for rotations up to 2.3% radians. This model considers 11 different geometric and material properties. Notably, to the best of the authors' knowledge, this is the only model that considers the bolt pre-tension force, P_t. Although the compiled database was large, the model constants (c_1 and c_2) were obtained based on regression analysis against only 13 tests (Ostrander 1970; Zoetemeijer and Kolstein 1975; Davison 1987). This is a limited number of data considering the number of regression constants.

Figure 18 shows the K_e and M_{ye} error scatter. Similar to previous models, this model is inconsistent and inaccurate in predicting the elastic stiffness, with several cases producing errors exceeding 50%. On the other hand, the model provides a reasonable estimate of M_{ye}, with a median error of -16% and +20% for stiffened and unstiffened connections. Interestingly, the model appears to show better and more consistent performance for stiffened connections, even though it was developed based on unstiffened specimen tests. Although this model considers several key features, its main drawback is the limited number of tests used in calibration. Hence, the full effect of these features is not captured. Other, more recent empirical models, that employed larger calibration data sets are shown to behave better as discussed later on.

$$\theta = c_2 \cdot \left(\frac{M}{c_1 - M} \right) \qquad \text{units: cm, kN} \tag{15}$$

Where,

$$\begin{aligned} c_1 &= h_{\mathrm{b}}^{0.8700} \cdot t_{\mathrm{ep}}^{0.917} \cdot t_{\mathrm{cf}}^{1.299} \cdot g^{-0.652} \cdot e_1^{-0.919} \cdot e_2^{-0.006} \cdot f_{\mathrm{y,P}}^{0.3790} \cdot f_{\mathrm{y,C}}^{2.0040} \cdot f_{\mathrm{y,B}}^{0.090} \cdot P_{\mathrm{y,\,bolt}}^{-0.233} \cdot P_t^{-0.240} \\ c_2 &= h_{\mathrm{b}}^{-2.385} \cdot t_{\mathrm{ep}}^{0.281} \cdot t_{\mathrm{cf}}^{0.631} \cdot g^{-0.013} \cdot e_1^{-0.561} \cdot e_2^{-0.270} \cdot f_{\mathrm{y,P}}^{-0.258} \cdot f_{\mathrm{y,C}}^{-0.234} \cdot f_{\mathrm{y,B}}^{0.643} \cdot P_{\mathrm{y,\,bolt}}^{0.2210} \cdot P_t^{0.3910} \end{aligned} \tag{15a}$$

With the advancement of 3-dimensional finite element (FE) simulation techniques within the structural engineering field, Bahaari and Sherbourne (1997) calibrated the Richard-Abbott four-parameter analytical model (refer to Figure 3b) against parametric FE simulations of 53 exterior EEPCs with and without column stiffeners. Empirical expressions are developed using nine geometric and two material features. Compared to previous models, the geometric features considered herein are inclusive of all components (column, beam, plate, and bolt). Equation (16a-d) shows these expressions for stiffened EEPCs (units are mm and MPa). This fitted model had a coefficient of determination, R^2, larger than 0.9. As demonstrated in Figure 6b, this model only does a reasonable job predicting the plastic strength of stiffened connections, with a median error of -11% and relatively low variability ($\sigma = \pm 34\%$). For the other response quantities, the mode predictions are unreliable. In particular, for unstiffened connections, the model appears to be highly sensitive to the column flange thickness, where this parameter is raised to an exponent that is an order of magnitude larger than the rest of the features. Unstiffened connections with t_{cf} <15mm appeared to result in very low strength. This is implied from Figure 6b where the minimum and 25 percentile error values approach -100%.

$$M_0 = t_{\mathrm{ep}}^{0.438} \cdot e_{\mathrm{rt}}^{0.726} \cdot t_{\mathrm{bw}}^{0.937} \cdot h_{\mathrm{b}}^{0.413} \cdot t_{\mathrm{cw}}^{1.914} \cdot b_{\mathrm{cf}}^{0.442} \cdot f_{\mathrm{y,P}}^{1.77} \cdot f_{\mathrm{y,b}}^{1.029} / (1319 \cdot (p_{\mathrm{t}} / d_{\mathrm{b}})^{0.88} \cdot t_{\mathrm{cf}}^{1.490}) \quad \leq 0.85 M_{\mathrm{p,b}} \tag{16a}$$

$$K_{\mathrm{e}} = e^{10.868} \cdot t_{\mathrm{ep}}^{0.450} \cdot e_{\mathrm{rt}}^{0.750} \cdot t_{\mathrm{bw}}^{2.488} \cdot h_{\mathrm{b}}^{0.061} \cdot t_{\mathrm{cf}}^{0.705} \cdot (g / d_{\mathrm{b}})^{0.233} / ((p_{\mathrm{t}} / d_{\mathrm{b}})^{0.330} \cdot d_{\mathrm{b}}^{0.710} \cdot b_{\mathrm{cf}}^{1.46}) \tag{16b}$$

$$K_{\mathrm{p}} = t_{\mathrm{ep}}^{0.450} \cdot h_{\mathrm{b}}^{5.100} \cdot t_{\mathrm{cf}}^{1.020} \cdot f_{\mathrm{y,B}}^{0.110} \cdot f_{\mathrm{y,P}}^{0.996} / ((g / d_{\mathrm{b}})^{3.970} (p_{\mathrm{t}} / d_{\mathrm{b}})^{1.180} \cdot d_{\mathrm{b}}^{8.330} \cdot t_{\mathrm{bw}}^{2.600}) \quad \leq 4\% K_e \tag{16b}$$

$$\eta = t_{\mathrm{ep}}^{0.130} \cdot e_{\mathrm{rt}}^{0.680} \cdot h_{\mathrm{b}}^{2.593} \cdot t_{\mathrm{cf}}^{0.210} \cdot f_{\mathrm{y,B}}^{0.160} / ((g / d_{\mathrm{b}})^{1.19} \cdot (p_{\mathrm{t}} / d_{\mathrm{b}})^{0.358} \cdot f_{\mathrm{y,P}}^{0.707} \cdot d_{\mathrm{b}}^{0.2.480} \cdot t_{\mathrm{bw}}^{2.750}) \tag{16d}$$

In a similar approach, Abolmaali et al. (2005) calibrated the Ramberg-Osgood model using the results of a parametric FE study involving 34 exterior FEPCs with a four-bolt configuration and stiffened column. Regression equations were developed to predict the three model parameters, as given by Eqns (17a-c). The model units are inches and psi. The equations consider nine features including the bolt layout, the end plate dimensions, the beam section dimensions, and the steel yield stress. While the model does not specify the yield stress of which component shall be used, that of the end plate is assumed herein given that end plate bending with the dominant deformation mode in these simulations.

Similar to Bahaari and Sherbourne (1997) model, this model yields large and inconsistent errors for K_{e} predictions as shown in Figure 19a. The model's main drawback is that it overlooks the column web and flange deformations and does not consider the bolt-pretension force; all of which have a significant effect on the elastic stiffness. This is why the model K_{e} estimates for stiffened beam-to-column and splice connections are relatively better than those for unstiffened connections. The model also does not consider connections with multiple bolt rows in tension which is common in practice. The model reference moment M_0 is compared herein with the deduced M_0. On average, the model does a better job estimating the plastic strength for both stiffened and unstiffened connections with a median error of +5% as shown in Figure 19b. Nonetheless, due to the aforementioned drawbacks, the model can reach a large error of ±50%.

$$M_0 = e^{0.5070} \cdot g^{-0.003} \cdot d_{\mathrm{b}}^{1.130} \cdot e_1^{0.448} \cdot b_{\mathrm{ep}}^{0.1390} \cdot t_{\mathrm{ep}}^{0.095} \cdot t_{\mathrm{bf}}^{0.1170} \cdot t_{\mathrm{bw}}^{0.1340} \cdot h_{\mathrm{b}}^{1.136} \cdot f_{\mathrm{y}}^{0.2960} \tag{17a}$$

$$\theta_0 = e^{-6.2660} \cdot g^{0.555} \cdot d_{\mathrm{b}}^{0.231} \cdot e_1^{2.938} \cdot b_{\mathrm{ep}}^{-0.499} \cdot t_{\mathrm{ep}}^{-0.563} \cdot t_{\mathrm{bf}}^{-0.080} \cdot t_{\mathrm{bw}}^{-0.485} \cdot h_{\mathrm{b}}^{-1.102} \cdot f_{\mathrm{y}}^{-0.062} \tag{17b}$$

$$\eta = e^{16.3150} \cdot g^{0.077} \cdot d_{\mathrm{b}}^{0.974} \cdot e_1^{0.946} \cdot b_{\mathrm{ep}}^{-1.009} \cdot t_{\mathrm{ep}}^{-0.478} \cdot t_{\mathrm{bf}}^{-0.287} \cdot t_{\mathrm{bw}}^{-0.451} \cdot h_{\mathrm{b}}^{0.011} \cdot f_{\mathrm{y}}^{-1.363} \tag{17c}$$

With the increased accessibility to computational power in the past decade. Rölle (2013) was able to conduct larger parametric FE simulations (164 FEPC and 68 EEPC exterior beam-to-column specimens). The generated data was then used to developed a semi-empirical model to determine the stiffness and strength of FEPCs and EEPCs. The model determines the connection plastic strength as the product of an empirical correction factor c, the bolt tensile strength F_{ub}, and the inner lever arm z (as defined in CEN (2005b)). Similarly, the elastic stiffness is computed as the product of several geometric features and further corrected using three empirical factors. The geometric features were chosen considering their correlation with the response parameters based on the simulation results. The empirical correction factors were regressed against the FE simulation data. The model performance with respect to K_e predictions is consistent with the rest of the models discussed so far, with mostly overestimated values (μ=+50%) and large inconsistency (σ >150%) in prediction errors (refer to Figure 6a). The model plastic strength predictions are consistent with small standard deviation, though the predictions are conservatively shifted by about 18% and 58% for FEPCs and EEPCs, respectively. The larger error for EEPCs is partially attributed to an additional 0.75 reduction factor employed by the model to consider the bolt pre-tension load effect on force distribution. Similar to many of the other models, simple amplification factors can be used to shift the model median errors to zero.

$$M_{\mathrm{p}} = c\, F_{\mathrm{ub}}\, z, \ \text{ where } c = 1.95\, \frac{t_{\mathrm{ep}}\, t_{\mathrm{cf}}\, f_{\mathrm{yP}}}{m\, m_2\, f_{\mathrm{ub}}} \tag{18a}$$

$$K_{\mathrm{e}} = \frac{t_{\mathrm{ep}}\, t_{\mathrm{cf}}\, h_{\mathrm{b}}}{c_1 \left(\dfrac{m}{4.5 d_{\mathrm{b}}}\right)^{c_2} \left(\dfrac{m_{\mathrm{ep}}}{2 d_{\mathrm{b}}}\right)^{c_3}} \quad \text{where } \begin{cases} c_1 = 7.0 \quad c_2 = 1.0 \quad c_3 = 0.25 \quad \text{for FEPC} \\ c_1 = 3.1 \quad c_2 = 0.5 \quad c_3 = 0.50 \quad \text{for EEPC} \end{cases} \tag{18b}$$

Most recently, Eladly and Schafer (2021) conducted parametric FE simulations of 160 different EEPC configurations with stiffened columns, fabricated from austenitic stainless steel. The study covered connections with stiffened columns, end plates with/without ribs, shallow beams, and thin end plates (t_{ep}<12mm, h_b<300mm, and d_b<16mm). The parametric results were then used to fit nonlinear regression models for each of the four Richard-Abbott model parameters (refer to Figure 3b). The model features include six geometric and three material parameters, as shown in Eqn (20). The model authors showed that this model is robust, yielding an average error of about 4% for the connection strength, but this was associated with large variability that reached 25% for the elastic stiffness and plastic strength parameters. Although the employed FE approach was validated against test data, the model was not benchmarked directly against test data.

Figure 20**Error! Reference source not found.**a-b shows the error in predicting K_e and M_0 with respect to the corresponding parameters deduced from the test data. In this figure, to be consistent with the model connection configuration, only connections with stiffened columns, two-bolt per row and single bolt row in the extended tension portion are considered. With respect to K_e, the model mostly predicts lower stiffness values. The predictions exhibit large variability consistent with prior observations for all the other models. Interestingly, on average, the model predictions for carbon steel connections (μ=-25%) are better than that of stainless steel connections (μ=-68%). The underestimated K_e values can be attributed to the fact that this model does not consider the strength/grade of the bolt or its pre-tension force. In fact, bolt pre-tension was not considered in the FE simulations used to develop this model. This can have a major effect on K_e (Hellquist 1966; Jenkins et al. 1986; Prescott 1987; Chasten 1988). Moreover, part of the observed error is due to the negligence of column web shear deformations. Particularly, in EEPCs with stiffened columns, insignificant deformations due to column flange bending are expected. On the other hand, the continuity plates do not restrain the column web-panel zone from deforming in shear. Therefore, one would expect that the model herein should have included the column web thickness rather than the column flange thickness.

With respect to M_0, the model underpredicts stainless steel connections' strength by about 28%. Similar to K_e, the model appears to do better (on average) for carbon steel connections with a median error of -14%. The M_0 error for most of the tests falls between ±70% which is still large. This error is mainly related to the exclusion of the geometric features associated with column deformations. This is demonstrated in Figure 20c which shows the correlation between the error and the beam depth to end-plate thickness ratio. In particular, the model overestimates the strength for connections with low $h_b/t_{ep} < 11.5$. Those involve shallow beams and thick end plates where column panel zone shear deformations tend to control. On the other hand, the model tends to underestimate the strength of connections with deep beams and thin end plates ($h_b/t_{ep} > 17.5$) that are mainly controlled by higher-mode buckling of the end plate and buckling of beam flanges/web. Furthermore, although not included in Figure 20, the model also yields very large errors ($>$200%) in predicting the strength of connections experiencing beam flange/web buckling. Those are either connections with slender beams (i.e., class 3 or 4 as per CEN (2005a)) or connections falling within or near the fully-rigid category (i.e., occurrence of beam buckling) (Ryan 1999; Sumner III 2003; Jain 2015).

Finally, one should note here that the applicability of this model to carbon steel connections is valid since the empirical model already considers both the yield and ultimate yield stresses when determining the post-yield stiffness (K_s); hence, the amount of plastic strain hardening generated by the material is implicitly considered. In fact, excluding any errors in K_e or M_0, this model produces a comparable post-yield stiffness for both stainless and carbon steel specimens as shown in Figure 20d with a median error close to zero. Most K_s errors are within the ±50% range. Although this error is large, it can be deemed acceptable given that errors in K_s are not as detrimental –to design and structural analysis- as those in K_e and considering the state-of-practice where the post-yield stiffness is either ignored (as in bilinear models), assumed constant (e.g., by setting K_s = 2~3% K_e (Davison et al. 1987; Landolfo 2022; Zhao et al. 2021) or setting the M_{max}/M_{ye} ratio to 1.1~1.3 (Lignos and Krawinkler 2011; Elkady and Lignos 2014)), or inaccurately predicted in other continuous models (Frye and Morris 1975; Abolmaali et al. 2005). This is better demonstrated in Figure A.1 based on full-response comparisons.

$$K_{\mathrm{e}} = \begin{cases} e^{-11.298} \cdot t_{\mathrm{ep}}^{0.81} \cdot g^{-0.24} \cdot (h_{\mathrm{b}} - z_2)^{-0.129} \cdot (z_1 - h_{\mathrm{b}})^{0.152} \cdot h_{\mathrm{b}}^{2.664} \cdot d_{\mathrm{b}}^{0.955} \cdot f_{\mathrm{y},0.2}^{0.06} \cdot t_{\mathrm{cf}}^{0.305} \cdot E^{0.173} & \text{w/o ribs} \\ e^{-13.754} \cdot t_{\mathrm{ep}}^{0.51} \cdot g^{-0.20} \cdot (h_{\mathrm{b}} - z_2)^{-0.188} \cdot (z_1 - h_{\mathrm{b}})^{-0.02} \cdot h_{\mathrm{b}}^{1.893} \cdot d_{\mathrm{b}}^{0.774} \cdot f_{\mathrm{y},0.2}^{0.22} \cdot t_{\mathrm{stiff,P}}^{0.110} \cdot E^{0.769} & \text{w ribs} \end{cases} \tag{19a}$$

$$K_{\mathrm{s}} = \begin{cases} e^{-11.312} \cdot t_{\mathrm{ep}}^{0.39} \cdot g^{-0.25} \cdot (h_{\mathrm{b}} - z_2)^{-0.10} \cdot (z_1 - h_{\mathrm{b}})^{-0.125} \cdot h_{\mathrm{b}}^{2.852} \cdot d_{\mathrm{b}}^{0.643} \cdot f_{\mathrm{y},0.2}^{0.074} \cdot t_{\mathrm{cf}}^{0.225} \cdot f_{\mathrm{u}}^{0.021} & \text{w/o ribs} \\ e^{-9.1150} \cdot t_{\mathrm{ep}}^{0.85} \cdot g^{-0.31} \cdot (h_{\mathrm{b}} - z_2)^{-0.19} \cdot (z_1 - h_{\mathrm{b}})^{-0.191} \cdot h_{\mathrm{b}}^{2.426} \cdot d_{\mathrm{b}}^{0.319} \cdot f_{\mathrm{y},0.2}^{0.100} \cdot t_{\mathrm{stiff,P}}^{0.375} \cdot f_{\mathrm{u}}^{0.033} & \text{w ribs} \end{cases} \tag{19b}$$

$$M_0 = \begin{cases} e^{-8.123} \cdot t_{\mathrm{ep}}^{1.024} \cdot g^{-0.11} \cdot (h_{\mathrm{b}} - z_2)^{-0.127} \cdot (z_1 - h_{\mathrm{b}})^{0.180} \cdot h_{\mathrm{b}}^{1.045} \cdot d_{\mathrm{b}}^{1.171} \cdot f_{\mathrm{y},0.2}^{0.420} & \text{w/o ribs} \\ e^{-5.868} \cdot t_{\mathrm{ep}}^{0.553} \cdot g^{-0.04} \cdot h_{\mathrm{b}}^{0.714} \cdot d_{\mathrm{b}}^{1.310} \cdot f_{\mathrm{y},0.2}^{0.261} \cdot t_{\mathrm{stiff,P}}^{0.030} & \text{w ribs} \end{cases} \tag{19c}$$

Models for connection ductility

The connection's rotational ductility, as measured by the failure rotation, is one of the parameters that are key to the study of system-level robustness under extreme hazards, such as progressive collapse under impact/blast loads and sidesway collapse under strong seismic events. This response quantity is generally overlooked in the aforementioned models given the insufficient data. Within the past few years, emphasis was placed on developing empirical or probabilistic models to estimate steel connection failure. For semi-rigid end plate connections, only two models are found and discussed herein.

Ostrowski and Kozłowski (2017) developed an expression to estimate the ultimate rotation (i.e., at failure) for exterior stiffened FEPCs. The expression, given by Eqn. (20), is developed based on only 11 FE parametric simulations where failure is controlled by bolt rupture. The FE model was validated against test data conducted at the material, component (T-stub), and joint levels; though the number of validation specimens was limited particularly at the joint level. The simulated specimens involved an HEB300 column and HEA360 beam with 4-bolts, t_{ep}=10~20mm, d_1=50~90mm, g=120~180mm, and fully pre-tensioned M20 Gr. 10.9 bolts. Eqn. (20) implies that θ_{f} is inversely and directly proportional to the end-plate thickness and the bolt gauge length, respectively. This is logical given that stiffer thick end-plate connections undergo negligible rotations before bolt failure. Figure 21a shows the error scatter based on beam-to-column test specimens that failed by bolt rupture. Note here that a drawback of Eqn. (20) is that it may result in negative θ_{f} values because of the presence of a constant negative scalar term (i.e., -42.48). Those cases are ignored in Figure 21a. For specimens falling within the model range of applicability, the figure shows that the model predictions are highly variable regardless of the connection geometric layout, where θ_{f} is reasonably underestimated by about 30%. Although this level of error may be acceptable, the model still yields large variability in its predictions even for connections within its applicability range, with errors reaching -100% and +200%. This can be mainly attributed to the exclusion of the material parameters, particularly that of the bolt which is related to the bolt fracture strain. Though not plotted in **Error! Reference source not found.**a, it should be noted that large errors are observed for connections failing by bolt stripping or weld failure. For these cases, the model tends to overestimate the failure rotation since these are early unplanned failure modes. Similar observations with respect to splice specimens; those are generally designed with thick end-plates (>30mm) and experience insignificant deformations prior to failure (Srouji 1983; Hendrick 1985; Steurer 1999). Hence, these cases should be treated differently in future models.

More recently, Eladly and Schafer (2021) also developed an empirical formula for the ultimate (i.e., failure rotation, θ_f) of stainless steel EEPCs, using Eqn (21), as part of the continuous nonlinear model discussed earlier. Predicting ductility is of particularly importance in this model since it is one of the key advantages of stainless over carbon steel. Similar to Ostrowski and Kozłowski (2017), the equations are developed considering bolt rupture as the failure mode. Note here that in the parametric study, A-80 stainless steel bolts (equivalent to Gr. 8.8) were considered. In the compiled experimental database, only 7 stainless steel specimens reached failure. The prediction error for those is plotted in Figure 21b where a median error of +2% and a highest error of -30% are observed. This level of error can be considered acceptable given the overall sensitivity of θ_f to geometric, material, and loading parameters (Elkady 2022). In particular, the model herein does not consider the loading protocol (monotonic versus cyclic), the bolt grade (duplex versus austenitic), and the bolt shear-to-tension force ratio (Song et al. 2020); all of which can have a significant effect on θ_f. For connections with regular high-strength steel bolts, the model overestimates θ_f by about 67%. This is expected considering the higher ductility of stainless steel bolts; at least 50% larger than carbon steel counterparts (Song et al. 2020). On the other hand, for Grade 10.9 bolts, the model underestimates θ_f by about 50% since it was developed based on lower bolt grade.

$$\theta_{\mathrm{f}} = t_{\mathrm{ep}}^{-1.267} \cdot e_1^{1.044} \cdot g^{0.714} - 42.48 \tag{20}$$

$$\theta_{\mathrm{f}} = \begin{cases} e^{-0.497} \cdot t_{\mathrm{ep}}^{-1.005} \cdot t_{\mathrm{cf}}^{-0.298} \cdot g^{0.253} \cdot (h_{\mathrm{b}} - z_2)^{0.559} \cdot (z_1 - h_{\mathrm{b}})^{0.126} \cdot h_{\mathrm{b}}^{-1.033} \cdot d_{\mathrm{b}}^{1.21} \cdot f_{\mathrm{y},0.2}^{-0.10} & \text{unstiff.} \\ e^{0.599} \cdot t_{\mathrm{ep}}^{-1.030} \cdot t_{\mathrm{cf}}^{-0.317} \cdot g^{0.190} \cdot (h_{\mathrm{b}} - z_2)^{0.585} \cdot (z_1 - h_{\mathrm{b}})^{0.091} \cdot h_{\mathrm{b}}^{-1.122} \cdot d_{\mathrm{b}}^{1.42} \cdot f_{\mathrm{y},0.2}^{-0.17} \cdot t_{\mathrm{stiff,P}}^{-0.252} & \text{stiff.} \end{cases} \tag{21}$$

Summary and Conclusions

Semi-rigid end-plate moment connections are widely used in practice and have been the focus of great amount of international research through the years. Much of this research was concerned with developing models, using different approaches, that can capture the connections' elastic and elastoplastic behavior for design and analysis purposes. Contrary to full-strength connections, semi-rigid connections' behavior can be more complex and sensitive to multiple factors. The accuracy of existing models, in predicting the moment-rotation response -or the characteristic stiffness, strength, and ductility parameters- of semi-rigid flush and extended end-plate moment connections, is assessed in this study using a comprehensive experimental database of more than 1200 specimens. This is the first study to conduct such a broad experimental-based assessment of 16 models to highlight the strengths and weaknesses of the different models and pave the road towards the development of more robust ones. The main findings are summarized as follows:

- Regardless of the model type and the associated complexity, the available models fall short of achieving consistent accuracy in predicting key response parameters, usually with errors exceeding 100%. This can be mainly attributed to the fact that most models are developed based on simplified assumptions that do not account for all loading, material, and geometric parameters influencing the response or are based on test/simulation data with a limited range of testing parameters (e.g., boundary conditions, applied load history) and connection configurations (e.g., beam depth, angle thickness, bolt pretension force). Consequently, model extrapolation to other configurations can yield high errors.
- All models, assessed in this study, yield excessive (error>100%) and inconsistent (error range>±50%) estimates of the elastic rotational stiffness (refer to Figure 6a). This confirms past findings in the literature. For instance, on average, the most rigorous Eurocode 3 component method overestimates the stiffness of FEPCs and EEPCs by about 85%±140% and 85%±140%, respectively. Several simpler models achieved comparable and sometimes better (though mostly non-conservative) predictions. Multiple connection features need to be accounted for to predict the elastic stiffness which is a particularly sensitive response parameter. For example, except for one model, all available models ignore the bolt pretension force although it has been shown to have a major impact on the stiffness (Hellquist 1966; Faella et al. 1998).
- Available models generally do better job predicting the connections' plastic strength compared to the elastic stiffness with the majority of errors are between ±40% (refer to Figure 6b). Both the yield line and the component methods provide reasonable estimates (excluding outliers), though the latter tends to be conservative by about 20%. Better estimates are observed for FEPCs compared to EEPCs, which is expected given the addition deformation complexities in the latter. Most of the assessed analytical and empirical models provide consistent estimates (narrow error range within ±30%), as long as they are applied within their applicability/development range.
- Based on the current assessment, it was shown that simple correction factors can temporarily be employed to improve the plastic strength and elastic stiffness predictions of several models and shift the median or mean prediction error to zero. Some of these correction factors are correlated with key geometric parameters.
- Several key parameters that are shown to affect the connection response have been commonly ignored in prediction models. This includes: 1) load protocol effect, 2) material hardening, 3) end-plate rib stiffeners, 4) column and beam axial loads (Wald and Švarc 2001; da Silva et al. 2004), and 5) unbalanced bending and shear-to-moment ratio (Li et al. 1996; Waqas et al. 2019; Béland et al. 2020).

- Bilinear models ignore the connection's post-yield stiffness while most continuous nonlinear ones do not provide good predictions. This is a key response parameter, arising from plastic strain hardening, that affects nonlinear simulations concerned with ductility and collapse capacity. This needs to be carefully considered in future models.
- Current models for predicting the connection ductility are limited and require further development. The two models assessed herein showed unreliable predictions of the failure rotation that is solely controlled by bolt rupture. For this failure mode, models need to consider the effects of the loading protocol, the bolt shear-to-tension load ratio, and the bolt pre-tension force. For connections controlled by other failure modes such as bolt stripping, weld failure, and end-plate tearing, test-based probabilistic –rather than empirical- models may be more sensible.
- Empirical models are simpler and at the same time comparable in terms of accuracy to analytical and mechanical models. However, to improve their robustness, it is necessary to 1) include many features covering the contributions of all the deforming components, and 2) employ a large set of data (ideally from physical tests or thoroughly validated FE models).
- For models developed based on FE simulations, the FE modeling approach must be rigorously validated with available test data of connections with different characteristics, before conducting any parametric simulations. Otherwise, the FE model may be biased. This is particularly critical for studies focused on quantifying ductility and failure rotation.
- Most empirical models rely on data sets generated by FE simulations. Those relying on physical test data employ limited data sets covering a narrow band of the design space. The comprehensive experimental database compiled herein offers the opportunity for developing more robust empirical models.
- Semi-rigid connection response characteristics are dependent on the controlling deformation mode(s). These modes are in turn dependent on the joint location and type (beam-to-column versus beam-to-beam and exterior versus interior) and the connection column web and end-plate stiffening. As such, future models may need to be developed based on discrete categories related to the connection topology.
- The apparent complexity of semi-rigid end-plate connections' behavior and their dependency on a multitude of test, geometric, and material parameters support the case for employing machine learning (ML) algorithms -such as neural networks- to predict the connection response parameters. The literature has demonstrated the efficiency of ML algorithms in capturing complex physical structural problems compared to standard nonlinear expressions. These, however, require large datasets of high quality, similar to the one compiled herein.

Data Availability Statement

Some or all data, models, or code generated or used during the study are available in a repository online in accordance with funder data retention policies.

Acknowledgments

This work was conducted at the National Infrastructure Laboratory, University of Southampton (UoS). The authors gratefully acknowledge the financial support provided by UoS to the first author as part of his graduate research.

Notation

The following symbols are used in this paper:

A_b	beam cross-section area
A_{vc}	column web shear area
b_{cf}	column flange width
b_{ep}	end-plate width
d_b	bolt diameter
c	constants or regression coefficients
E_i	modulus of elasticity of component i [P: end plate, C: column, B: beam]
e	Euler number
e_c	end-plate extension at the compression side
e_f	effective end-plate length in bending ($e_f = e_t - e_{rt} + t_{bf}/2$)
e_{rc}	distance between the top bolt row and end-plate edge in compression
e_{rt}	distance between the top bolt row and end-plate edge in tension
e_t	end-plate extension at the tension side
e_i	vertical distance of bolt row i to the beam's tension-flange external edge
e_i	bolt horizontal edge distance on the end-plate length
F_{row}	strength of a given bolt row
F_{ub}	bolt ultimate strength
$f_{y,i}$	yield stress of component i [P: end plate, C: column, B: beam, b: bolt]
$f_{u,i}$	ultimate stress of component i [P: end plate, C: column, B: beam, b: bolt]
G	shear modulus
g	bolt gauge (distance between bolt columns)
h_b	beam depth
h_c	column depth
h_{ep}	end-plate depth
I_{ep}	end-plate cross-section second moment of inertia ($b_{ep}\, t_{ep}^3/12$)
$I_{x,b}$	beam second moment of inertia
K_{cws}	stiffness of column web in shear
K_e	initial elastic rotational stiffness
K_{epb}	stiffness of end-plate in bending
K_s	post-yield hardening stiffness based on an equal-area bilinear fit
$K_{s,tangent}$	post-yield hardening stiffness based on the tangent slope at M_{max}
k	regression coefficient
k_i	elastic stiffness coefficient for component i
L_b	beam length
l_a	lever arm

l_c	distance between the upper portion of the flush end plate and the horizontal plastic hinge
M_0	reference –plastic- moment based on the Ramberg-Osgood model
M_u	ultimate moment corresponding to 3% joint rotation
M_p	plastic moment
$M_{j,Rd}$	joint design –plastic- moment resistance as per CEN (2005b)
M_{max}	maximum moment developed by a joint during a test
M_y	yield moment
M_{ye}	equivalent yield moment based on an equal-area bilinear fit
m	vertical distance between the tension bolt center and the nearest tension beam flange edge
m_{cf}	horizontal distance between the bolt center and column flange fillet edge
m_{ep}	horizontal distance between the bolt center and beam web weld
P_f	bolt proof load
$P_{y,bolt}$	bolt yield load
P_t	bolt pre-tension load
p_f	distance from the tension bolt center to the center line of the beam tension flange
p_i	bolt row inner pitch
p_t	bolt row pitch above and below the tension flange
RP_{model}	response parameter predicted by a model
RP_{test}	response parameter deduced from test data
r_c	column fillet radius
$S_{j,ini}$	joint initial rotational stiffness as per CEN (2005b)
t_{bf}	beam flange thickness
t_{bw}	beam web thickness
t_{cf}	column flange thickness
t_{cw}	column web thickness
t_{ep}	end-plate thickness
$t_{stiff,C}$	column stiffener thickness
$t_{stiff,P}$	end-plate stiffener thickness
t_{weld}	fillet weld thickness
Y_{cf}	yield line parameter for the column flange
Y_{ep}	yield line parameter for the end-plate
$V_{ep,0}$	plastic shear force capacity per unit length
$V_{ep,u}$	ultimate shear force at the upper portion of the flush end plate $\bar{x}$
$\bar{x}$	mean error
$Z_{x,b}$	beam plastic section modulus
z_{ex}	arm length between extreme bolt rows
z_i	arm length between bolt row *i* and beam compression flange center
z_{row}	arm length between a given bolt row and the beam compression flange center
β	transformation parameter as per CEN (2005b)
ϵ	error metric
θ_{cd}	design rotation capacity
θ_u or θ_f	ultimate or failure rotation
θ_0	reference –plastic- rotation based on Ramberg-Osgood and the modified 3-parameter power models
σ	standard deviation of the error
μ	median error

References

Abdalla, K. M., and Chen, W.-F. (1995). "Expanded database of semi-rigid steel connections." *Computers & Structures*, 56(4), 553-564, DOI: 10.1016/0045-7949(94)00558-K.

Abolmaali, A., Matthys, J. H., Farooqi, M., and Choi, Y. (2005). "Development of moment–rotation model equations for flush end-plate connections." *Journal of Constructional Steel Research*, 61(12), 1595-1612, DOI: 10.1016/j.jcsr.2005.05.004.

Aggarwal, A. K. (1994). "Comparative tests on end plate beam-to-column connections." *Journal of Constructional Steel Research*, 30(2), 151-175, DOI: 10.1016/0143-974X(94)90048-5.

AISC (2016a). "Prequalified connections for special and intermediate steel moment frames for seismic applications." *ANSI/AISC 358-10*, Chicago, IL.

AISC (2016b). "Specification for structural steel buildings." *ANSI/AISC 360-16*, Chicago, IL.

Al-Aasam, H. (2013). "Modern engineering design: Analytical and numerical modelling of semi-rigid connections." Ph.D. Thesis, The University of Manchester, Manchester, UK.

Bahaari, M. R., and Sherbourne, A. N. (1997). "Finite element prediction of end plate bolted connection behavio ii: Analytic formulation." *Journal of Structural Engineering*, 123(2), 165-175, DOI: 10.1061/(ASCE)0733-9445(1997)123:2(165).

BCSA (2021). "Uk structural steelwork: 2050 decarbonisation roadmap."London, UK.

Béland, T., Tremblay, R., Hines, E. M., and Fahnestock, L. A. (2020). "Full-scale cyclic rotation and shear-load testing of double web with top and seat angle beam-column connections." *Journal of Structural Engineering*, 146(8), 04020164, DOI: 10.1061/(ASCE)ST.1943-541X.0002685.

Benterkia, Z. (1991). "End-plate connections and analysis of semi-rigid steel frames." Ph.D. Thesis, University of Warwick, Coventry, UK.

Bræstrup, M. W. (1970). "Yield-line theory and limit analysis of plates and slabs." *Magazine of Concrete Research*, 22(71), 99-106, DOI: 10.1680/macr.1970.22.71.99.

Brown, N. D. (1995). "Aspects of sway frame design and ductility of composite end plate connections." Ph.D. Thesis, University of Warwick, Coventry, United Kingdom.

Brown, N. D., Hughes, A. F., and Anderson, D. (2001). "Prediction of the initial stiffness of ductile end-plate steel connections." *Proceedings of the Institution of Civil Engineers - Structures and Buildings*, 146(1), 17-29, DOI: 10.1680/stbu.2001.146.1.17.

Celik, H. K., and Sakar, G. (2022). "Semi-rigid connections in steel structures: State-of-the-art report on modelling, analysis and design." *Steel and Composite Structures*, 45(1), 1-21, DOI: 10.12989/scs.202.

CEN (1998). "Eurocode 3, Part 1-1 revised Annex J: Joints in building frames." *1993-1-1: 1992/A2: 1998*, Brussels, Belgium.

CEN (2005a). "Eurocode 3 - design of steel structures, part 1-1: General rules and rules for buildings." *BS-EN 1993-1-1-2006*, Brussels, Belgium.

CEN (2005b). "Eurocode 3 - design of steel structures, part 1-8: Design of joints." *BS-EN 1993-1-8-2006*, Brussels, Belgium.

Chasten, C. P. (1988). "Theoretical modeling and testing of 8-bolt extended end-plate connections." M.Sc. Thesis, Lehigh University, Pennsylvania, USA.

Chen, W. F., Kishi, N., and Komuro, M. (2011). *Semi-rigid connections handbook*, J. Ross Publishing Inc., Florida, USA.

Coelho, A. M. G., and Bijlaard, F. S. K. (2007). "Experimental behaviour of high strength steel end-plate connections." *Journal of Constructional Steel Research*, 63(9), 1228-1240, DOI: 10.1016/j.jcsr.2006.11.010.

D'Alessandro, E., Brando, G., and De Matteis, G. (2018). "Design charts for end-plate beam-to-column steel joints." *Proceedings of the Institution of Civil Engineers - Structures and Buildings*, 171(6), 444-462, DOI: 10.1680/jstbu.16.00203.

da Silva, L. S., de Lima, L. R. O., da Vellasco, P. C. G., and de Andrade, S. A. L. (2004). "Behaviour of flush end-plate beam-to-column joints under bending and axial force." *Steel and Composite Structures*, 4(2), 77-94, DOI: 10.12989/SCS.2004.4.2.077.

Davison, J. B. (1987). "Strength of beam-columns in flexibly connected steel frames." Ph.D. Thesis, University of Sheffield, Sheffield, England.

Davison, J. B., Kirby, P. A., and Nethercot, D. A. (1987). "Rotational stiffness characteristics of steel beam-to-column connections." *Journal of Constructional Steel Research*, 8(1), 17-54, DOI: 10.1016/0143-974X(87)90052-6.

Demonceau, J.-F., Weynand, K., Jaspart, J.-P., and Müller, C. (2010). "Application of Eurocode 3 to steel connections with four bolts per horizontal row." *Proc., Stability and Ductility of Steel Structures (SDSS) Conference* Rio de Janeiro, Brazil, 199.

Díaz, C., Martí, P., Victoria, M., and Querin, O. M. (2011). "Review on the modelling of joint behaviour in steel frames." *Journal of Constructional Steel Research*, 67(5), 741-758, DOI: 10.1016/j.jcsr.2010.12.014.

Drucker, D. C. (1956). "The effect of shear on the plastic bending of beams." *Journal of Applied Mechanics*, 23(4), 509-514, DOI: 10.1115/1.4011392.

Dubina, D., Ciutina, A., and Stratan, A. (2001). "Cyclic tests of double-sided beam-to-column joints." *Journal of Structural Engineering*, 127(2), 129-136, DOI: 10.1061/(ASCE)0733-9445(2001)127:2(129).

Eatherton, M. R., Nguyen, T. N., and Murray, T. M. (2021). "Yield line patterns for end-plate moment connections." *Report No. CE/VPI-ST-21/05*, Virginia Polytechnic Institute and State University, Blacksburg, VA, USA.

Eladly, M. M., and Schafer, B. W. (2021). "Numerical and analytical study of stainless steel beam-to-column extended end-plate connections." *Engineering Structures*, 240, 112392, DOI: 10.1016/j.engstruct.2021.112392.

Elkady, A. (2022). "Response characteristics of flush end-plate connections." *Engineering Structures*, 269, DOI: 10.1016/j.engstruct.2022.114856.

Elkady, A., and Lignos, D. G. (2014). "Modeling of the composite action in fully restrained beam-to-column connections: implications in the seismic design and collapse capacity of steel special moment frames." *Earthquake Engineering & Structural Dynamics*, 43(13), 1935-1954, DOI: 10.1002/eqe.2430.

Faella, C., Piluso, V., and Rizzano, G. (1998). "Experimental analysis of bolted connections: Snug versus preloaded bolts." *Journal of Structural Engineering*, 124(7), 765-774, DOI: 10.1061/(ASCE)0733-9445(1998)124:7(765).

Frye, M. J., and Morris, G. A. (1975). "Analysis of flexibly connected steel frames." *Canadian Journal of Civil Engineering*, 2(3), 280-291, DOI: 10.1139/l75-026.

Gao, J. D., Du, X. X., Yuan, H. X., and Theofanous, M. (2021). "Hysteretic performance of stainless steel double extended end-plate beam-to-column joints subject to cyclic loading." *Thin-Walled Structures*, 164, 107787, DOI: 10.1016/j.tws.2021.107787.

Gao, J. D., Yuan, H. X., Du, X. X., Hu, X. B., and Theofanous, M. (2020). "Structural behaviour of stainless steel double extended end-plate beam-to-column joints under monotonic loading." *Thin-Walled Structures*, 151, 106743, DOI: 10.1016/j.tws.2020.106743.

Goldberg, J. E., and Richard, R. M. (1963). "Analysis of nonlinear structures." *Journal of the Structural Division*, 89(4), 333-351, DOI: 10.1061/JSDEAG.0000948.

Goverdhan, A. V. (1984). "A collection of experimental moment-rotation curves and evaluation of predicting equation for semi-rigid connections." Ph.D. Thesis, Vanderbilt University, Nashville, Tennessee.

Guo, B., Wang, L., Wang, Y., Shi, Y., and Tian, H. (2011). "Experimental study on rotational stiffness of steel frame beam-column connections." *Journal of Building Structures*, 32(10), 82-89, DOI:

Hellquist, T. I. (1966). "The behaviour of end plate connections." M.Sc. Thesis, University of Saskatchewan, Saskatchewan, Canada.

Hendrick, D. M. (1985). "Unification of flush end-plate design procedures." Ph.D. Thesis, University of Oklahoma, Oklahoma, USA.

Heong, T. T. (2003). "Design appraisal of steel-concrete composite joints." Ph.D. Thesis, National University of Singapore, Singapore.

Hettula, P. (2017). "Moment-rotation response of a flush end-plate splice." M.Sc. Thesis, Aalto university, Espoo, Finland.

Jain, N. (2015). "Developing and validating new bolted end-plate moment connection configurations." M.Sc. Thesis, Virginia Polytechnic Institute and State University, Virginia, USA.

Jaspart, J. (1991). "Study of the semi-rigidity of beam-to-column joints and its influence on the resistance and stability of steel buildings." Ph.D. Thesis, Liège University, Wallonia, Belgium.

Jenkins, W. M., Tong, C. S., and Prescott, A. T. (1986). "Moment-transmitting end-plate connections in steel construction, and a proposed basis for flush endplate design." *The Structural Engineer*, 64A(5), 121-132, DOI:

Johnson, L. G., Cannon, J. C., and Spooner, L. A. (1960). "High tensile preloaded bolted joints for development of full plastic moments." *British. Welding Journal*, 7, 560-569, DOI:

Jones, L. L., and Wood, R. H. (1967). *Yield-line analysis of slabs*, Thames & Hudson and Chatto & Windus, London, UK.

Kidd, M., Judge, R., and Jones, S. W. (2016). "Current uk trends in the use of simple and/or semi-rigid steel connections." *Case Studies in Structural Engineering*, 6, 63-75, DOI: 10.1016/j.csse.2016.05.004.

Kong, Z., Hong, S., Vu, Q.-V., Cao, X., Kim, S.-E., and Yu, B. (2020). "New equations for predicting initial stiffness and ultimate moment of flush end-plate connections." *Journal of Constructional Steel Research*, 175, 106336, DOI: 10.1016/j.jcsr.2020.106336.

Kozlowski, A., Kowalczyk, R., and Gizejowski, M. (2008). "Estimation of the initial stiffness and moment resistance of steel and composite joints." *Proc., 8th World Congress, Council on Tall Buildings and Urban Habitat (CTBUH)*, Dubai, United Arab Emirates.

Kukreti, A. R., Murray, T. M., and Abolmaali, A. (1987). "End-plate connection moment-rotation relationship." *Journal of Constructional Steel Research*, 8(1), 137-157, DOI: 10.1016/0143-974X(87)90057-5.

Landolfo, R. (2022). " European seismic prequalification of steel beam-to-column joints: EQUALJOINTS and EQUALJOINTS-Plus projects." *Journal of Constructional Steel Research*, 192(1), DOI: 10.1016/j.jcsr.2022.107238.

Li, T. Q., Nethercot, D. A., and Choo, B. S. (1996). "Behaviour of flush end-plate composite connections with unbalanced moment and variable shear/moment ratios—II. Prediction of moment capacity." *Journal of Constructional Steel Research*, 38(2), 165-198, DOI: 10.1016/0143-974X(96)00016-8.

Liew, J. Y. R., Heong, T. T., and Shanmugam, N. E. (2004). "Composite joints subject to reversal of loading—Part 1: Experimental study." *Journal of Constructional Steel Research*, 60(2), 221-246, DOI: 10.1016/j.jcsr.2003.08.010.

Lignos, D. G., Hartloper, A., Elkady, A., Deierlein, G. G., and Hamburger, R. (2019). "Proposed updates to the ASCE 41 nonlinear modeling parameters for wide-flange steel columns in support of performance-based seismic engineering." *Journal of Structural Engineering*, 145(9), 04019083, DOI: 10.1061/(ASCE)ST.1943-541X.0002353.

Lignos, D. G., and Krawinkler, H. (2011). "Deterioration modeling of steel components in support of collapse prediction of steel moment frames under earthquake loading." *Journal of Structural Engineering*, 137(11), 1291-1302, DOI: 10.1061/(ASCE)ST.1943-541X.0000376.

Luo, L., Du, M., Yuan, J., Shi, J., Yu, S., and Zhang, Y. (2020). "Parametric analysis and stiffness investigation of extended end-plate connection." *Materials*, 13(22), 5133, DOI:

Mak, L., and Elkady, A. (2021). "Experimental database for steel flush end-plate connections." *Journal of Structural Engineering*, 147(7), 04721006, DOI: 10.1061/(ASCE)ST.1943-541X.0003064.

Mirza, O., and Uy, B. (2011). "Behaviour of composite beam–column flush end-plate connections subjected to low-probability, high-consequence loading." *Engineering Structures*, 33(2), 647-662, DOI: 10.1016/j.engstruct.2010.11.024.

Murray, T. M., and Shoemaker, W. L. (2002). "Flush and extended multiple-row moment end-plate connections." *Design Guide 16*, American Institute of Steel Construction, Chicago, Illinois, USA.

Murray, T. M., and Sumner, E. A. (2003). "Extended end-plate moment connections: Seismic and wind applications." *Design Guide 4*, American Institute of Steel Construction, Chicago, Illinois, USA.

Nethercot, D. A. (1984). "Steel beam to column connections - A review of test data and their applicability to the evaluation of the joint behaviour of the performance of steel frames." *Report No. RR1084*, University of Sheffield, Sheffield, UK.

NIST/ATC (2018). "Recommended modeling parameters and acceptance criteria for nonlinear analysis in support of seismic evaluation, retrofit, and design" *NIST GCR 17-917-45*, Prepared for the U.S. Department of Commerce and the National Institute of Standards and Technology (NIST) by the Applied Technology Council (ATC).

Nogueiro, P., da Silva, L. S., Bento, R., and Simões, R. (2009). "Calibration of model parameters for the cyclic response of end-plate beam-to-column steel-concrete composite joints." *Steel and Composite Structures*, 9, 39-58, DOI: 10.12989/scs.2009.9.1.039

Ostrander, J. R. (1970). "An experimental investigation of end plate connections." M.Sc. Thesis, University of Saskatchewan, Saskatchewan, Canada.

Ostrowski, K., and Kozłowski, A. (2017). "Rotation capacity of bolted flush end-plate stiffened beam-to-column connection." *Civil and Environmental Engineering Reports*, 25(2), 173-184, DOI: 10.1515/ceer-2017-0028.

Packer, J. A., and Morris, L. J. (1977). "A limit state design method for the tension region of bolted beam-column connections." *The Structural Engineer*, 55(10), DOI:

Patnana, V., Vyavahare, A. Y., and Gupta, L. M. (2019). "Moment–rotation response for semi-rigid connections." *Recent advances in structural engineering, volume 1*, Springer, 313-326.

Prescott, A. T. (1987). "The performance of end-plate connections in steel structures and their influence on overall structural behaviour." Ph.D. Thesis, Hatfield Polytechnic, Hatfield, UK.

Qiang, X., Bijlaard, F. S. K., Kolstein, H., and Jiang, X. (2014). "Behaviour of beam-to-column high strength steel endplate connections under fire conditions – Part 1: Experimental study." *Engineering Structures*, 64, 23-38, DOI: 10.1016/j.engstruct.2014.01.028.

Ramberg, W., and Osgood, W. R. (1943). "Description of stress-strain curves by three parameters." *Report No. NACA-TN-902*, National Advisory Committee for Aeronautics, Washington, D.C, USA.

Richard, R. M., and Abbott, B. J. (1975). "Versatile elastic-plastic stress-strain formula." *Journal of the Engineering Mechanics Division*, 101(4), 511-515, DOI: 10.1061/JMCEA3.0002047.

Rölle, L. (2013). "The load-bearing and deformation behavior of bolted steel and composite joints in fully plastic design and in extraordinary design situations (in german)." Ph.D. Thesis, University of Stuttgart, Stuttgart, Germany.

Ryan, J. C. (1999). "Evaluation of extended end-plate moment connections under seismic loading." M.Sc. Thesis, Virginia Polytechnic Institute and State University, Virginia, USA.

SCI/BCSA (2013). "Joints in steel construction: Moment-resisting joints to Eurocode 3." *Publication P398*, The Steel Construction Institute & The British Constructional Steelwork Association Limited, London, UK.

Sherbourne, A. N. (1961). "Bolted beam-to-column connections." *The Structural Engineer*, 39(6), 203-210, DOI:

Shi, G., Shi, Y., and Wang, Y. (2007). "Behaviour of end-plate moment connections under earthquake loading." *Engineering Structures*, 29(5), 703-716, DOI: 10.1016/j.engstruct.2006.06.016.

Skiadopoulos, A., Elkady, A., and Lignos, D. G. (2021). "Proposed panel zone model for seismic design of steel moment-resisting frames." *Journal of Structural Engineering*, 147(4), 04021006, DOI: 10.1061/(ASCE)ST.1943-541X.0002935.

Sommer, W. H. (1969). "Behaviour of welded header plate connections." University of Toronto.

Song, Y., Wang, J., Uy, B., and Li, D. (2020). "Stainless steel bolts subjected to combined tension and shear: Behaviour and design." *Journal of Constructional Steel Research*, 170, 106122, DOI: 10.1016/j.jcsr.2020.106122.

Srouji, R. (1983). "Yield-line analysis of end-plate connections with bolt force predictions." M.Sc. Thesis, University of Oklahoma, Oklahoma, USA.

Steenhuis, M., Jaspart, J.-P., Gomes, F., and Leino, T. (1998). "Application of the component method to steel joints." *Proc., Control of the Semi-Rigid Behaviour of Civil Engineering Structural Connections Conference*, Liege, Belgium, pp 125-143.

Steurer, A. (1999). "The load-bearing behavior and rotational capacity of bolted end plate connections (in german)." *IBK Bericht*, 247, DOI: 10.3929/ethz-a-003878456.

Sumner III, E. A. (2003). "Unified design of extended end-plate moment connections subject to cyclic loading." Ph.D. Thesis, Virginia Polytechnic Institute and State University, Virginia, USA.

Tahir, M. M., Shahrin, M., Tahya, N., Abd Rahman, A. B., and Saad, S. (2006). "Economic aspects of the use of partial and full strength joints on multi-storey unbraced steel frames." Report No. 74109, Universiti Teknologi Malaysia, Johor Bahru, Malaysia.

Tahir, M. M., Hussein, M. A., Sulaiman, A., and Mohamed, S. (2009). "Comparison of component method with experimental tests for flush end-plate connections using hot-rolled perwaja steel sections." *International Journal of Steel Structures*, 9(2), 161-174, DOI: 10.1007/BF03249491.

Terracciano, G. (2013). "Yield and ultimate rotations of beam-to-column end-plate connections." Ph.D. thesis, University of Naples Federico II, Naples, Italy.

Terracciano, G., Della Corte, G., Di Lorenzo, G., and Landolfo, R. (2018). "Design tools for bolted end-plate beam-to-column joints." *Journal of Engineering*, 2018, 9689453, DOI: 10.1155/2018/9689453.

Thomson, A. W., and Broderick, B. M. (2002). "Earthquake resistance of flush end-plate steel joints for moment frames." *Proceedings of the Institution of Civil Engineers, Structures and Buildings*, 152(2), 157-165, DOI: 10.1680/stbu.2002.152.2.157.

Ungermann, D., Schneider, S., Feldmann, M., Müller, C., Oberegge, O., Hockelmann, H.-P., and Ritterbursch, N. (2009). "Development of a design model for bolted, moment-bearing end plate connections with 4 bolts in a bolt row based on en 1993-1-8: 2003 (in german)." *AiF-Projekt 15059 N/2*, AiF.

Vértes, K., and Iványi, M. (2005). "Investigation of minor axis and 3D bolted end-plate connections-experimental and numerical analysis-load tests." *Periodica Polytechnica Civil Engineering*, 49(1), pp. 47-58.

Wald, F., and Švarc, M. (2001). "Experiments with end plate joints subject to moment and normal force." *CTU Report 2-3 - Contributions to Experimental Investigation of Engineering Materials and Structures*, Czech Technical University in Prague, Prague, Czech Republic, pp. 1-13.

Waqas, R., Uy, B., and Thai, H.-T. (2019). "Experimental and numerical behaviour of blind bolted flush endplate composite connections." *Journal of Constructional Steel Research*, 153, 179-195, DOI: 10.1016/j.jcsr.2018.10.012.

Weynand, K., Jaspart, J.-P., and Steenhuis, M. (1996). "The stiffness model of revised annex J of Eurocode 3." *Connections in steel structures iii*, Elsevier, 441-452.

Weynand, K., Jaspart, J.-P., and Steenhuis, M. (1998). "Economy studies of steel building frames with semi-rigid joints." Proc., Journal of Constructional Steel Research, 85(1).

Youngson, G. K. (2002). "Behaviour of unstiffened column webs in bolted beam-to-column connections in building frames." Ph.D. Thesis, University of Abertay Dundee, Dundee, Scotland.

Zhao, X., He, S., and Yan, S. (2021). "Full-range behaviour of t-stubs with various yield line patterns." *Journal of Constructional Steel Research*, 186, 106919, DOI: 10.1016/j.jcsr.2021.106919.

Zoetemeijer, P. (1974). "A design method for the tension side of statically loaded, bolted beam-to-column connections." *HERON*, 20(1).

Zoetemeijer, P. (1981). "Semi-rigid bolted beam-to-column connections with stiffened column flanges and flush-end plates." *Proc., Joints in Structural Steel Works, Pentech Press*, Teesside Polytechnic, UK, 2.99-92.118.

Zoetemeijer, P., and Kolstein, M. H. (1975). "Bolted beam-column connections with short end plate." University of Technology Delft, Delft, Netherlands.

Table 1. Summary of existing predictive models for bare steel semi-rigid end-plate moment connections with I-shaped columns in chronological order

Reference	Model type	Predictions	Applicability
Frye and Morris (1975)	Empirical	Full M-θ	FEPC/EEPCs
Kukreti et al. (1987)	Empirical	Full M-θ	Splice FEPCs
Benterkia (1991)	Empirical	Full M-θ	Unstiffened FEPCs
Bahaari and Sherbourne (1997)	Empirical	Full M-θ	EEPCs
Brown et al. (2001)	Analytical	K_e	FEPCs/ EEPCs
Murray and Shoemaker (2002)	Analytical	M_p	FEPCs/EEPCs
CEN (2005b)	Analytical/Mechanical	K_e and M_p	All connection types
Abolmaali et al. (2005)	Empirical	Full M-θ	Stiffened FEPCs
Kozlowski et al. (2008)	Empirical	K_e and M_p	FEPCs/EEPCs
Guo et al. (2011)	Analytical	K_e	EEPCs
Rölle (2013)	Semi-Empirical	K_e and M_p	FEPCs/EEPCs
Ostrowski and Kozłowski (2017)	Empirical	θ_u	Stiffened FEPCs
Terracciano et al. (2018)	Empirical	K_e and M_p	Splice EEPCs
Kong et al. (2020)	Semi-Empirical	K_e and M_u	FEPCs
Luo et al. (2020)	Analytical	K_e	Stiffened EEPCs
Eladly and Schafer (2021)	Empirical	Full M-θ	Stainless EEPCs

Table A.1. Summary of observed error metrics

Model reference	Parameter	Connection type	Error metrics [%] μ	$\bar{x}$	σ	[*min* *max*]
Frye and Morris (1975)	K_e	FEPC-stiffened	−88	−86	±11	[-100 -44]
		FEPC-unstiffened	−23	−16	±61	[-98 +300]
		EEPC-stiffened	−28	+3	±95	[-93 +351]
		EEPC-unstiffened	+9	+60	±166	[-97 +752]
	M_p	FEPC-stiffened	−85	−80	±12	[-94 -25]
		FEPC-unstiffened	+13	+55	±132	[-89 +495]
		EEPC-stiffened	−39	−32	±32	[-80 +90]
		EEPC-unstiffened	+160	+209	±209	[-67 +697]
Kukreti et al. (1987)	K_e	FEPC-splice/int. stiff.	+178	+295	±361	[-66 +1635]
Benterkia (1991)	K_e	FEPC-stiffened	−10	+26	±80	[-78 +242]
		FEPC-unstiffened	+101	+186	±216	[-31 +930]
	M_p	FEPC-stiffened	−17	−4	±35	[-51 +90]
		FEPC-unstiffened	+18	+27	±51	[-57 +171]
Bahaari and Sherbourne (1997)		EEPC-stiffened	+151	+176	±163	[-66 +724]
		EEPC-unstiffened	+29	+157	±31	[-100 +1236]
		EEPC-stiffened	−12	−5	±34	[-56 +130]
		EEPC-unstiffened	−33	−29	±62	[-100 +172]
Yield line method	M_p	FEPC	+2	+1	±27	[-59 +60]
		EEPC	+2	+4	±38	[-86 +144]
Brown et al. (2001)	K_e	FEPC	−45	−12	±90	[-99 +409]
		EEPC	−64	−50	±57	[-99 +252]
CEN (2005b)	$S_{j,ini}$	FEPC	+1	+19	±75	[-94 +286]
		EEPC	+53	+85	±142	[-97 +657]
	$M_{j,Rd}$	FEPC	−9	−3	±36	[-70 +177]
		EEPC	−20	−15	±32	[-90 +201]
Abolmaali et al. (2005)	K_e	FEPC-stiffened	+19	+44	±98	[-86 +385]
		FEPC-unstiffened	+180	+269	±253	[-87 +950]
	M_0	FEPC-stiffened	+0	+4	±47	[-51 +172]
		FEPC-unstiffened	+8	+16	±45	[-53 +180]
Kozlowski et al. (2008)	K_e	FEPC-inside range	+53	+92	±120	[-89 +411]
		FEPC-outside range	+38	+54	±89	[-76 +364]
		EEPC-inside range	+129	+198	±262	[-93 +1191]
		EEPC-outside range	+78	+145	±215	[-98 +951]
	M_p	FEPC-inside range	−6	−1	±36	[-55 +87]
		FEPC-outside range	−12	−9	±32	[-59 +81]
		EEPC-inside range	−45	−39	±28	[-91 +54]
		EEPC-outside range	−41	−35	±25	[-77 +30]
Guo et al. (2011)	K_e	EEPC	−36	−2	±111	[-99 +666]
Rölle (2013)	K_e	FEPC	+64	+144	±230	[-92 +1057]
		EEPC	+41	+101	±185	[-85 +1392]
	M_p	FEPC	−18	−9	±35	[-60 +94]
		EEPC	−58	−55	±15	[-84 +7]
Ostrowski and Kozłowski (2017)	θ_f	FEPC-inside range	+20	+26	±86	[-87 +191]
		FEPC-outside range	−26	−24	±56	[-99 +137]
Terracciano et al. (2018)	K_e	EEPC-stiffened	− 20	+10	±46	[-71 +147]
		EEPC-Unstiffened	−9	+30	±104	[-98 +388]
	M_p	EEPC-Stiffened	+29	+24	±25	[-24 +67]
		EEPC-Unstiffened	+54	+74	±84	[-84 +356]
Kong et al. (2020)	K_e	FEPC-Stiffened	−51	−49	±23	[-87 +16]
		FEPC-Unstiffened	−34	−28	±89	[-94 +285]

	M_u	FEPC-Stiffened	+9	+14	±29	[-54 +96]
		FEPC-Unstiffened	+33	+54	±70	[-38 +269]
Eladly and Schafer (2021)	K_e	EEPC-Stainless steel	−68	−42	±52	[-82 +68]
		EEPC-Carbon steel	−26	−2	±75	[-94 +378]
	M_0	EEPC-Stainless steel	−28	−24	±20	[-60 +5]
		EEPC-Carbon steel	−14	−6	±31	[-52 +123]
	θ_u	EEPC-Stainless steel	+2	−13	±26	[-53 +9]
		EEPC-Carbon steel	+67	+66	±114	[-58 +413]

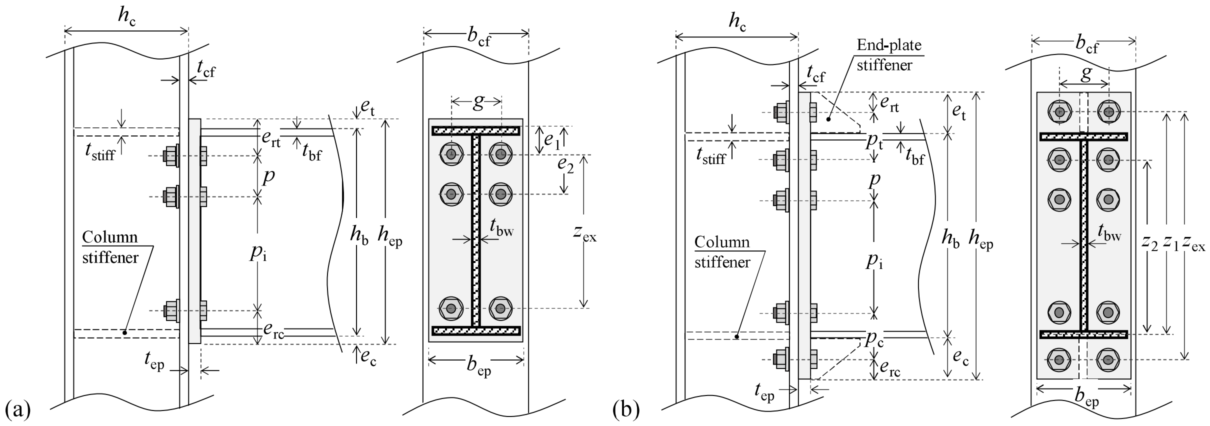

Figure 1. Geometric parameters for (a) flush and (b) extended end-plate connections

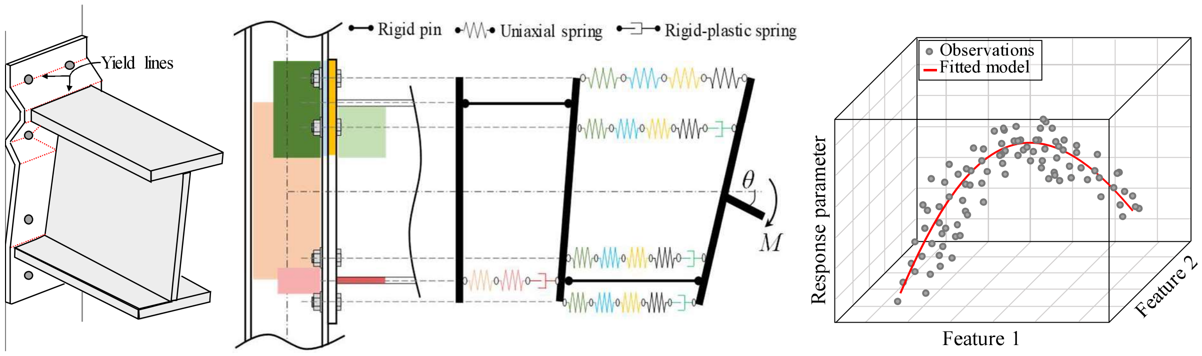

1148 Figure 2. Illustration of main numerical model types: (a) analytical [yield line method adapted from Eatherton et al. (2021)], (b)
1149 mechanical, and (c) empirical

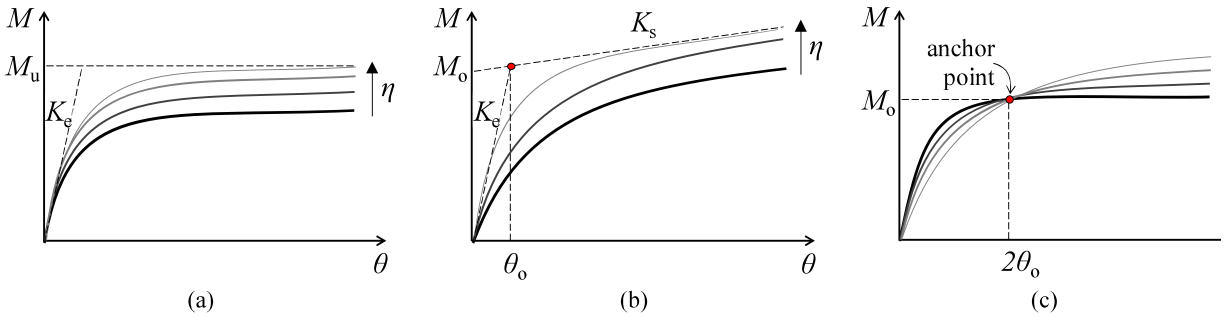

Figure 3. Common nonlinear models: (a) Modified three-parameter power model; (b) Modified four-parameter power model; (c) Ramberg-Osgood model

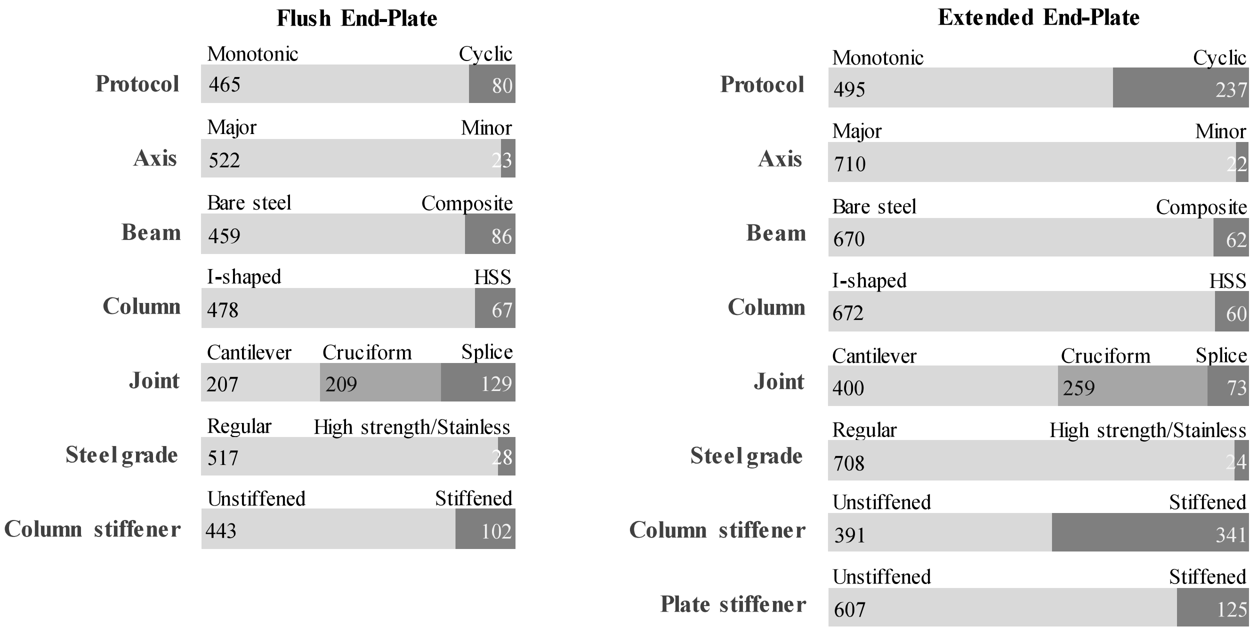

Figure 4. Summary breakdown of the collected experimental database

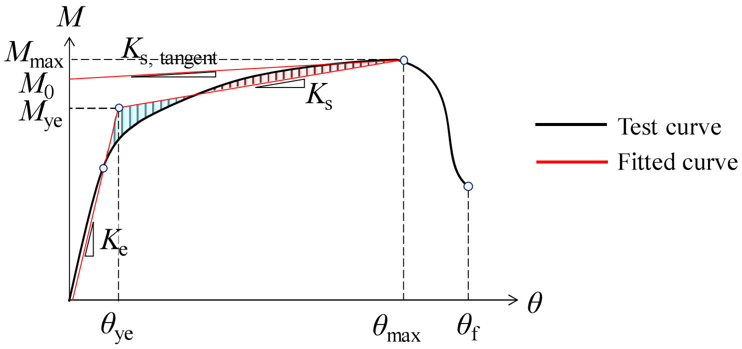

Figure 5. Bi-linear fitting of the moment-rotation response

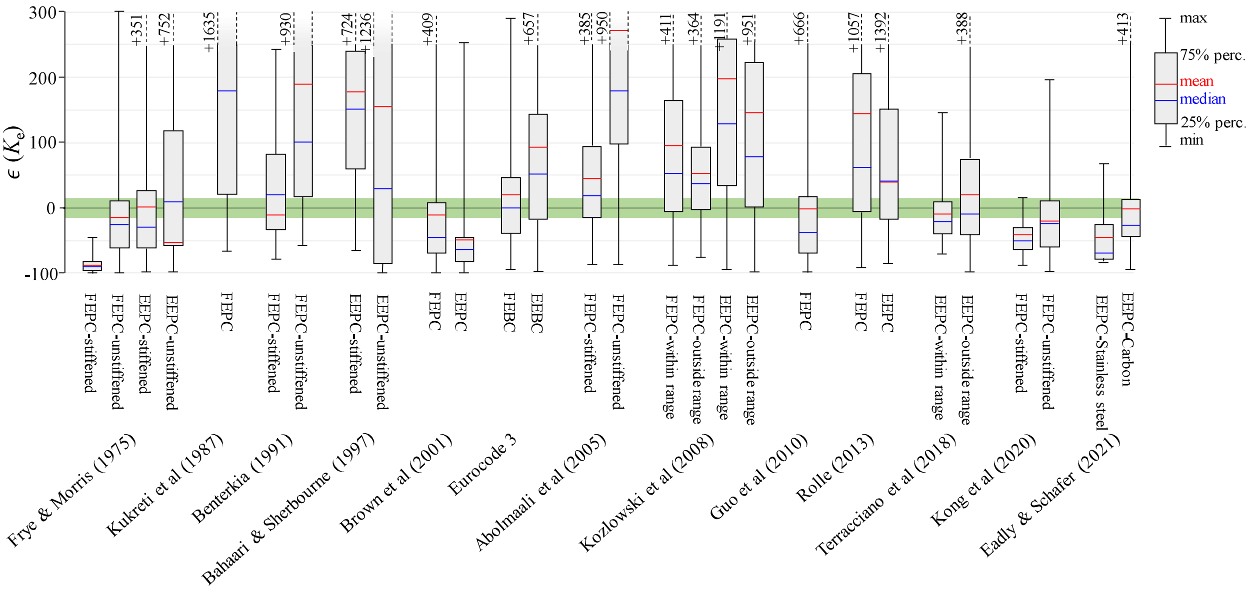

(a)

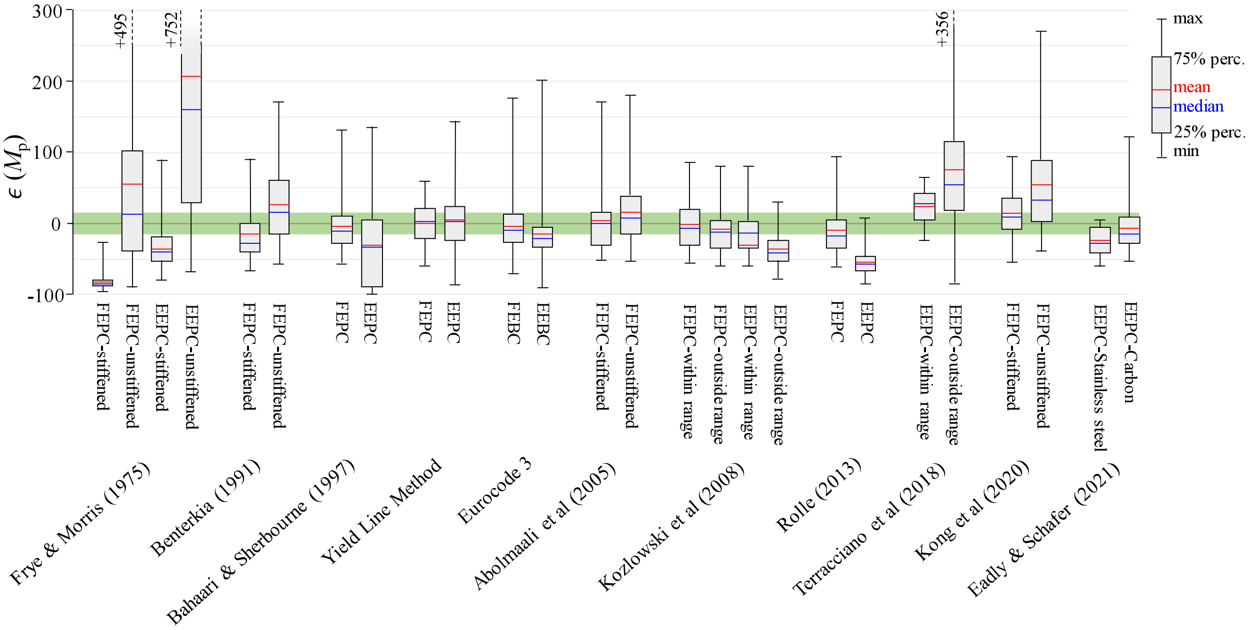

(b)

Figure 6. Statistical summary of (a) elastic stiffness and (b) plastic strength errors for the assessed prediction models [green band represents ±15% error range]

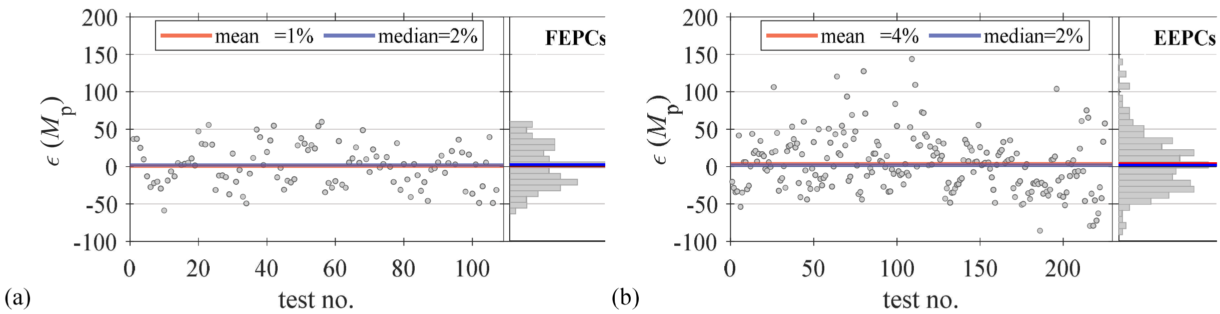

Figure 7. Yield line method: M_p error for (a) FEPCs and (b) EEPCs

Figure 8 Click here to access/download;Figure;Figure_8.pdf

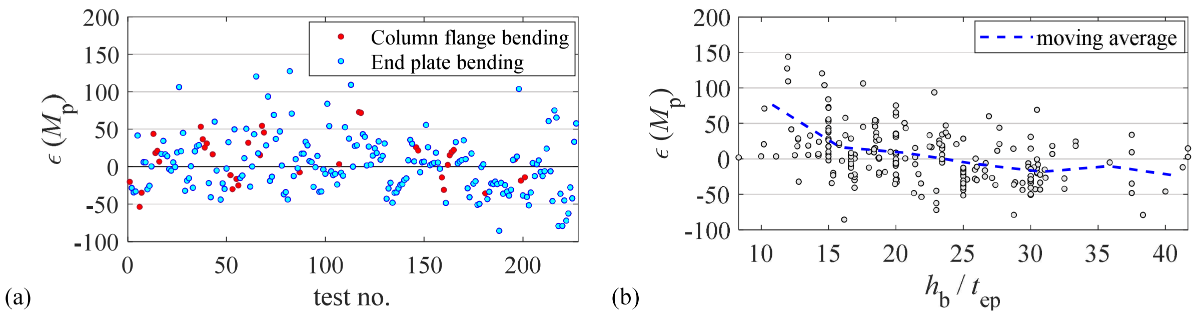

1164 Figure 8. Yield line method: M_p error dependency on (a) the deforming component and (b) the beam height to plate thickness
1165 ratio

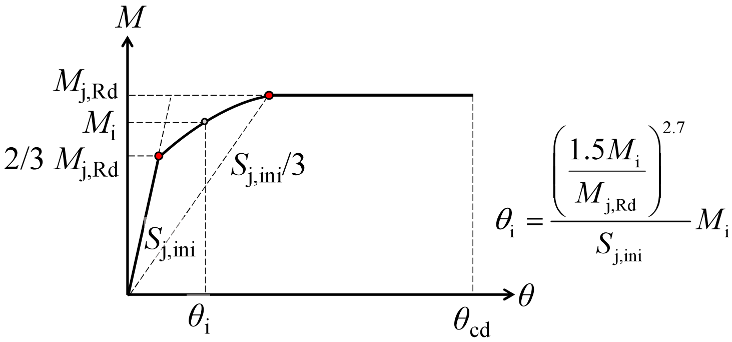

Figure 9. Moment-rotation curve for semi-rigid bolted connections per Eurocode 3, Part 1-8

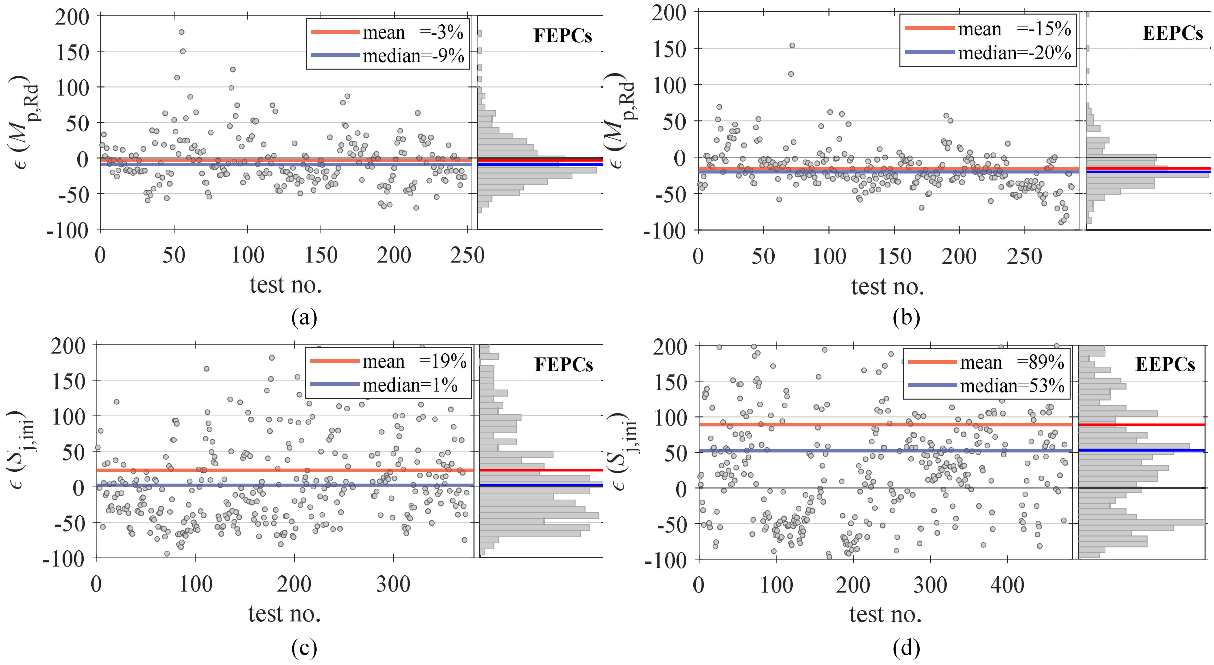

1168 Figure 10. Eurocode 3 component method: $M_{p,Rd}$ error for (a) FEPCs and (b) EEPCs; $S_{j,ini}$ error for (c) FEPCs and (d) EEPCs

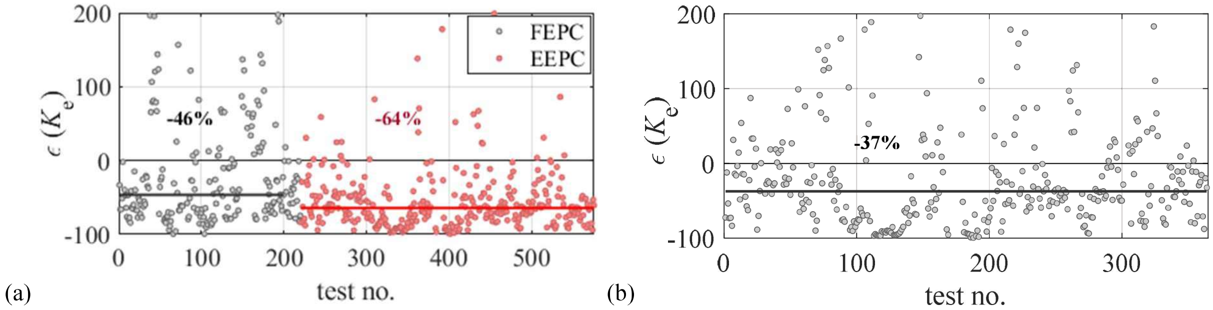

Figure 11. K_e error based on: (a) Brown et al. (2001) and (b) Guo et al. (2011)

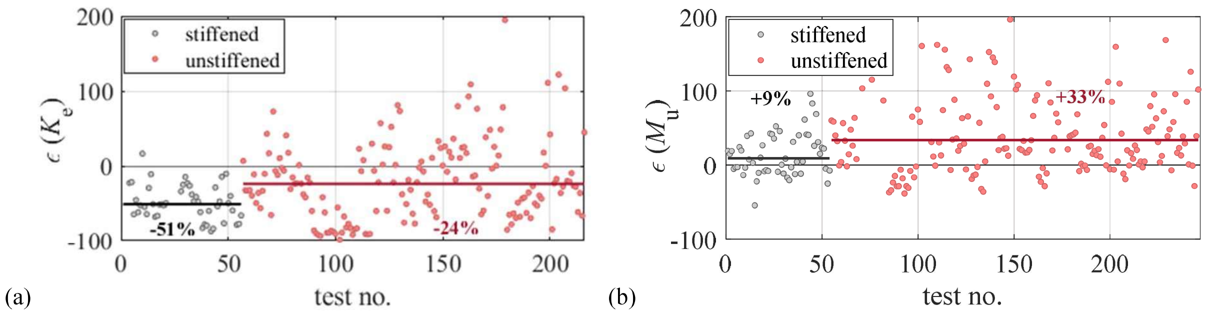

Figure 12. Kong et al. (2020) model for FEPCs: (a) K_e error; (b) M_u error

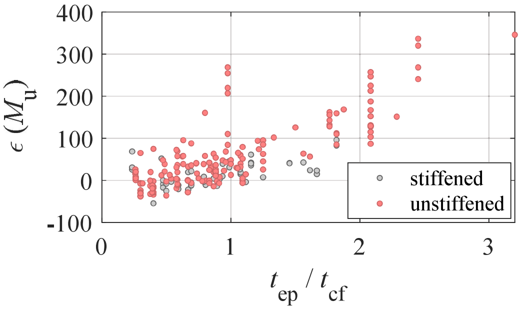

1171
1172 Figure 13. Kong et al. (2020) model for FEPCs: correlation between M_u error and t_{ep}/t_{cf}

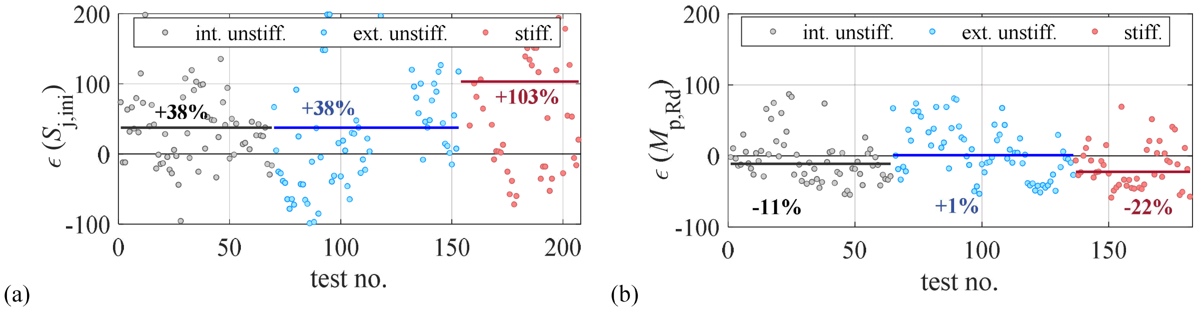

1173 Figure 14. Kozlowski et al. (2008) model for FEPCs: (a) K_e and (b) M_p error

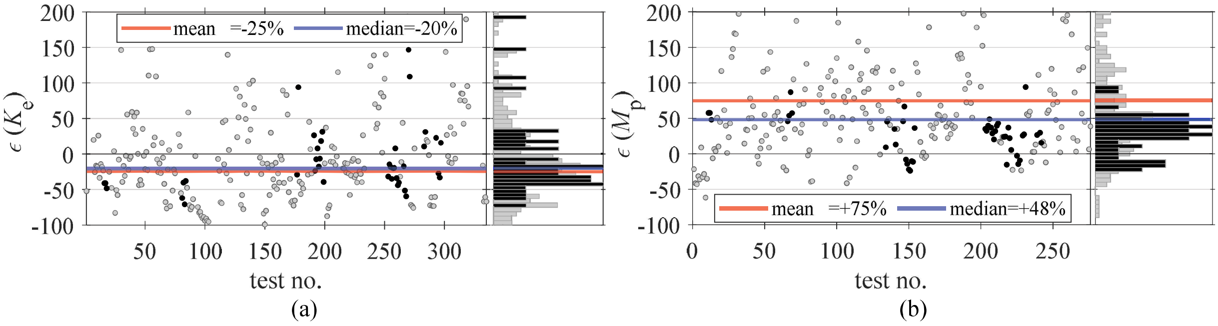

1174 Figure 15. Terracciano et al. (2018) model: (a) K_e error; (b) M_p error for EEPCs

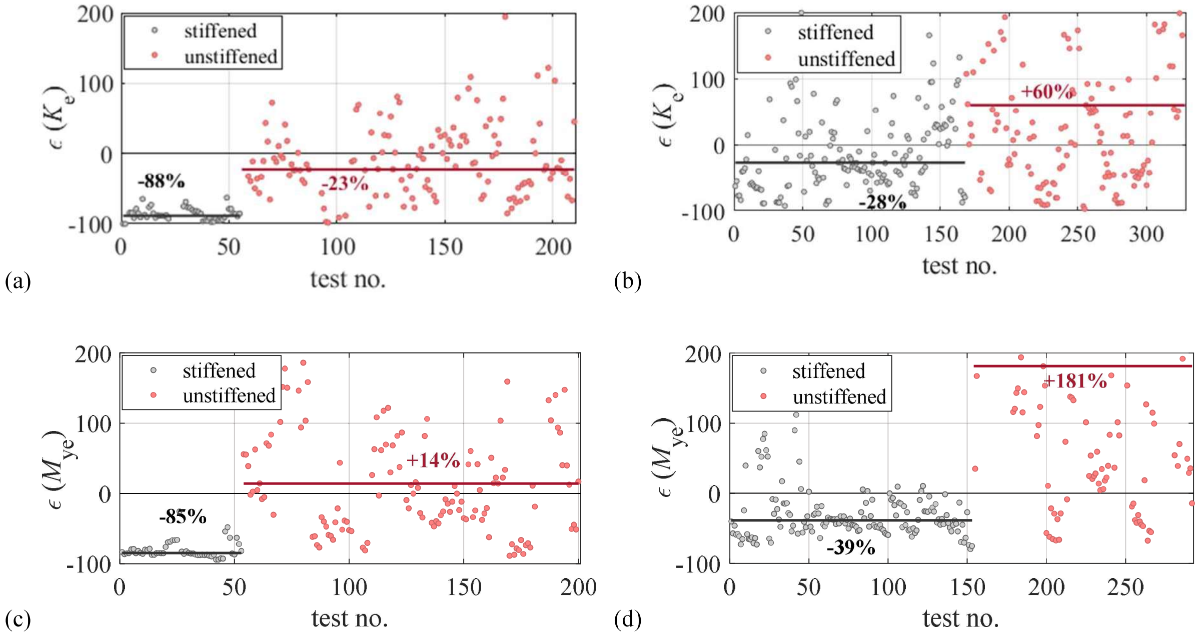

Figure 16. Frye and Morris (1975) model: K_e error for (a) FEPC and (b) EEPC; M_{ye} error for (c) FEPC and (d) EEPC

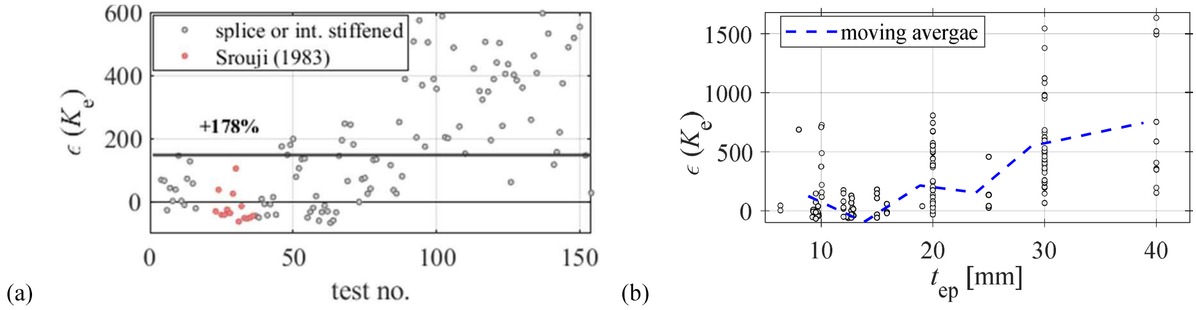

Figure 17. Kukreti et al. (1987) model for FEPCs: (a) error in predicting K_e; (b) correlation between K_e error and end-plate thickness

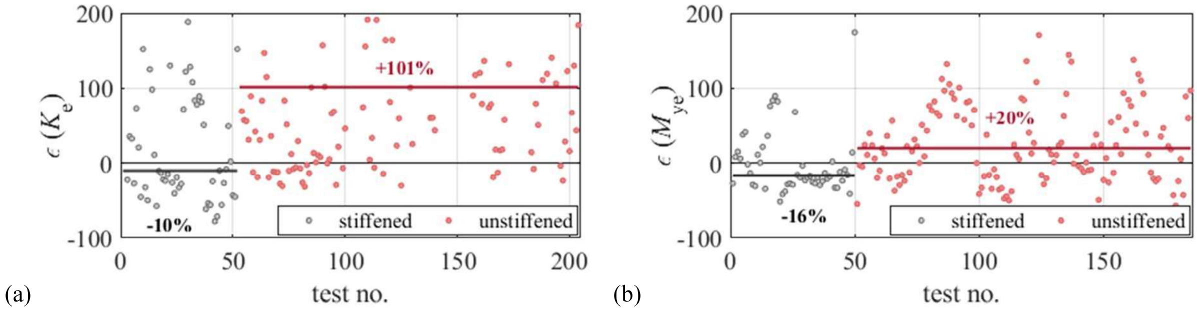

1178 Figure 18. Benterkia (1991) model for FEPCs: (a) K_e error; (b) M_{ye} error

Figure 19

Click here to access/download;Figure;Figure_19.pdf

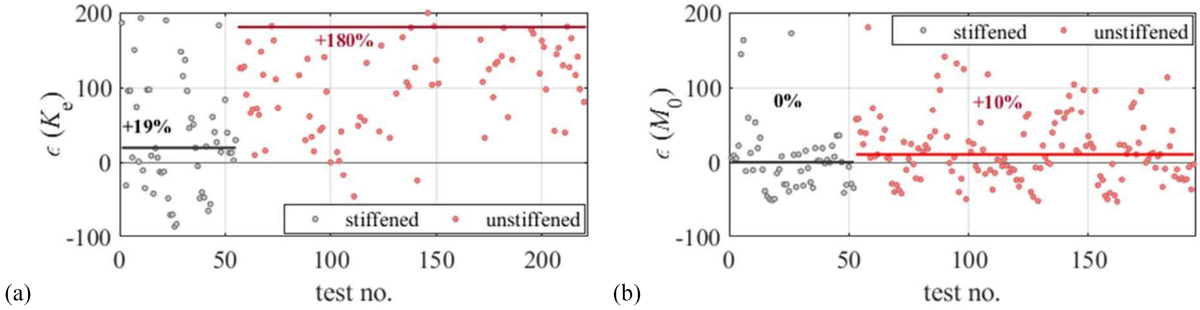

1179 Figure 19. Abolmaali et al. (2005) model for EEPCs: (a) K_e error; (b) M_0 error

Figure 20 Click here to access/download;Figure;Figure_20.pdf

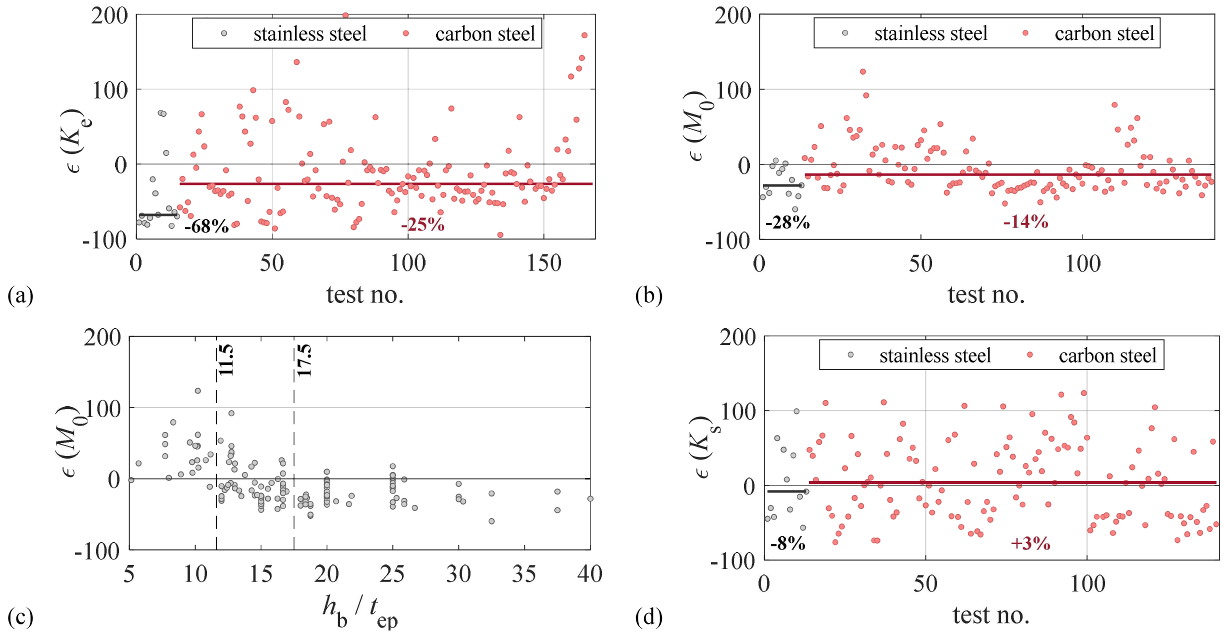

1180 Figure 20. Eladly and Schafer (2021) model for EEPCs: (a) K_e error; (b) M_0 error; (c) M_0 error versus h_b/t_{ep}; (d) K_s error

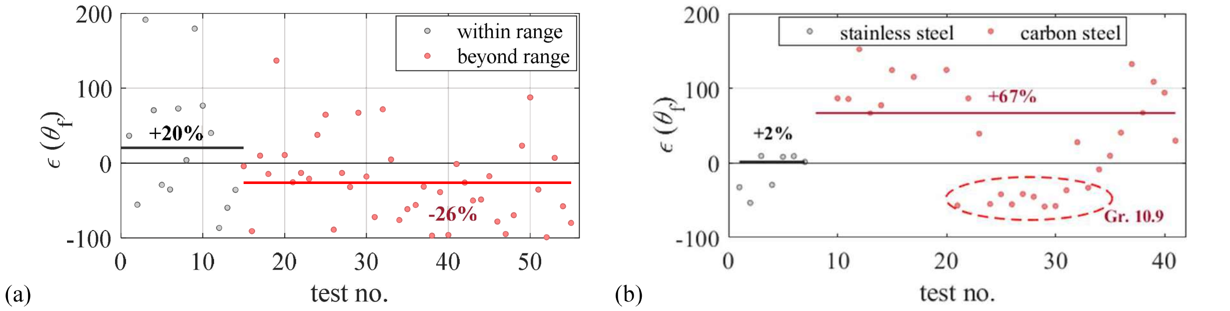

Figure 21. Error in predicting failure rotation based on empirical models by (a) Ostrowski and Kozłowski (2017) for FEPCs and (b) Eladly and Schafer (2021) for EEPCs

Appendix

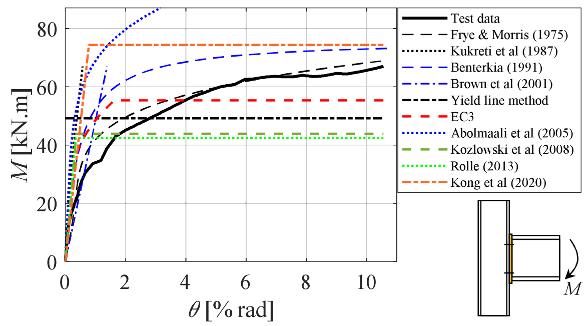

(a) Specimen FEP1 by Tahir et al. (2009)

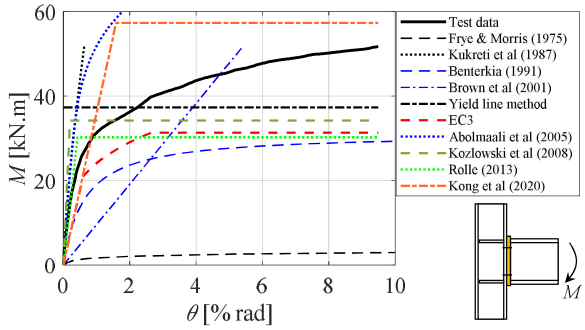

(b) Specimen C2 by Aggarwal (1994)

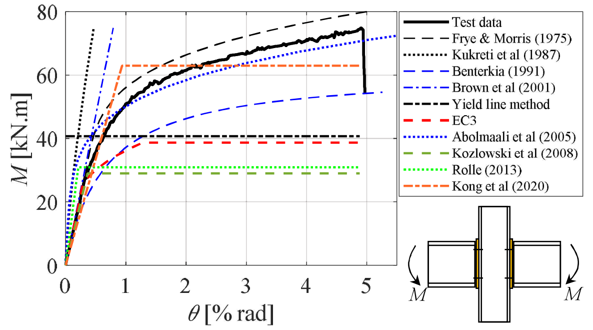

(c) Specimen R2-12 by Vértes and Iványi (2005)

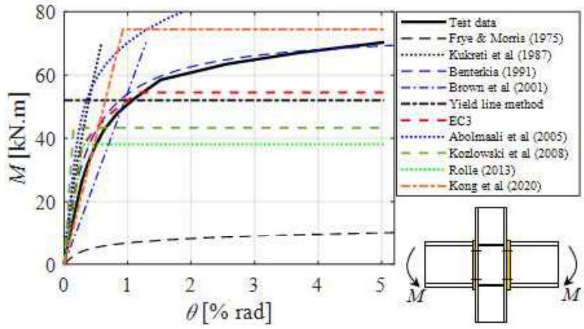

(d) Specimen 2 by Ostrander (1970)

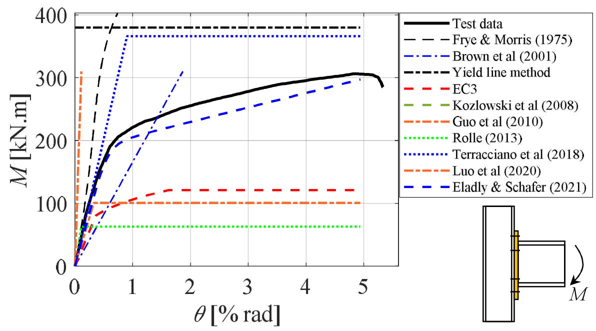

(e) Specimen JD4-M by Shi et al. (2007)

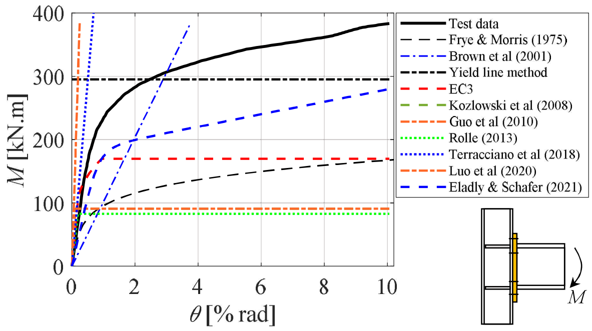

(f) Specimen J4-1 by Nogueiro et al. (2009)

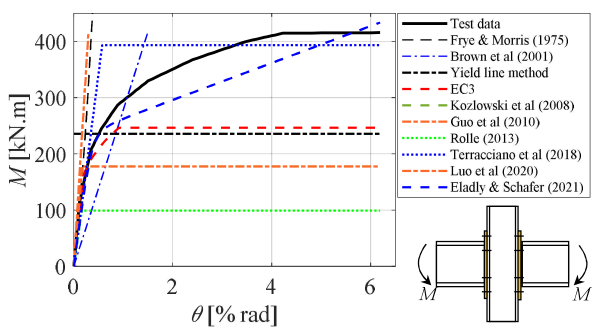

(g) Specimen T4 by Youngson (2002)

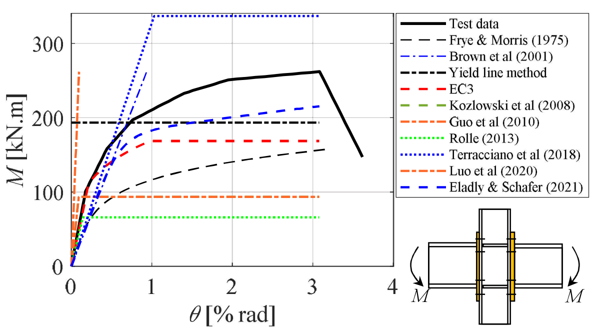

(h) Specimen BX-SS-M by Dubina et al. (2001)

Figure A.1. Sample comparisons of existing models' predictions with reference test data

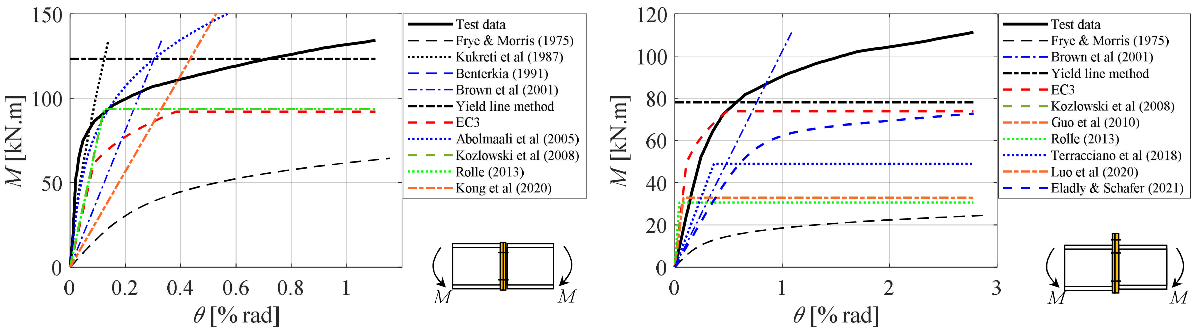

(i) Specimen F1-3/4-1/2-16 by Srouji (1983)

(j) Specimen 11K by Steurer (1999)

Figure A.1. Sample comparisons of existing models' predictions with reference test data (continued)